CHAPTER 2

THE ASSOCIATION BETWEEN PULSARS AND SUPERNOVA REMNANTS

In this chapter we shall discuss the following question:

> **Why is the association between pulsars and supernova remnants so poor ?**

Although nearly 500 pulsars and 150 supernova remnants are known, only in four cases is there a physical association between them. The small number of the observed associations is usually attributed to various selection effects, including beaming, which work against the detection of pulsars. However. the synchrotron nebulae these pulsars are expected to produce would not suffer from these selection effects, and should therefore be detectable. But the fraction of such nebulae among the known supernova remnants is less than $\sim 10\%$. Radhakrishnan and Srinivasan (1980) had suggested that this may be understood if there are neutron stars in all supernova remnants, but they are not functioning as pulsars. This suggestion has been restated more recently by other authors (e.g. Blandford, Applegate and Hernquist 1983).

We shall, in this chapter, take the point of view that supernova remnants not only contain neutron stars but they function as pulsars, but most of these pulsars are unable to produce detectable nebulae. Although there may be several possible reasons why an active pulsar may not produce a plerionic 'nebula like the Crab nebula, we argue that the most likely reason is that:

Most pulsars are born as slow rotators

CONTENTS

CHAPTER 2

THE ASSOCIATION BETWEEN PULSARS AND [illegible] REMNANTS

CHAPTER 2

ASSOCIATION BETWEEN SUPERNOVA REMNANTS AND PULSARS

2.1 INTRODUCTION AND BACKGROUND

The idea that neutron stars are born in supernovae dates back to the classic paper by Baade and Zwicky (1934). Subsequent theoretical studies of stellar evolution have shown that the formation of a neutron star is probably the mechanism for at least the supernovae of type II. Young neutron stars function as pulsars, and supernovae leave behind supernova remnants. Thus one would expect an association between them. Interestingly, independent estimates of the supernova rate, the rate of formation of pulsars and the birthrate of supernova remnants agree reasonably well with each other.

The Supernova Rate

One of the most reliable ways of estimating the supernova rate in our Galaxy is by using the Historical records. This has been done by Clark and Stephenson (1977a,b). They obtain

a rate of about one in ~20 years.

Another method that can be employed is to observe supernovae occurring in external galaxies similar to ours in morphology and dimensions. A statistical analysis of these observations can yield the average rate of occurrence of supernovae per galaxy. One may then assume that the same average supernova rate applies also to our Galaxy. Tamrnann (1982) obtains a rate of one in ~25 years using this method.

The study of supernovae occurring in external galaxies also yields the relative frequency of Type I and Type II supernovae. In galaxies like ours, these rates are roughly equal (Tammann 1982), which implies a Galactic SNII rate of one in – 30-50 yr.

The Pulsar Birthrate

An estimate of Galactic pulsar birthrate from the observed sample of pulsars involves two steps: The first is to obtain the total number of active pulsars in the Galaxy, allowing for selection effects such as a minimum detectable flux, pulse smearing due to dispersion in the interstellar medium, pulsar luminosity as a function of its period and magnetic field, beaming factor and so on. The second step is to obtain the rate of evolution of pulsars using their measured slowdown rates. If one assumes that the pulsar population has reached a steady state, then one can estimate the rate of pulsar births necessary for maintaining such a

population. The most recent estimates of the pulsar birthrate lie in the range of one in 30-50 yr (Vivekanand and Narayan 1981; Lyne, Manchester and Taylor 1985; Narayan 1987).

Recently Blaauw (1985; 1987) has estimated the birthrate of pulsars by using a slightly different approach. Using the observed pulsars lying within a distance of ~ 1 kpc from the sun, he computes a "local" birthrate of pulsars by adopting an average lifetime of 4.6 million years for the pulsars, as suggested by the most recent analysis (Lyne, Manchester and Taylor 1985). The advantage of restricting oneself to this small region is that one can be reasonably confident that within it the sample of pulsars is complete. Blaauw's results indicate that the "local" birthrate of pulsars should be

$$33/f \text{ pulsars per kpc}^2 \text{ per } 4.6 \text{ Myr}$$

where f is the "average beaming factor", which gives the probability of the observer to be within the emission cone of a pulsar. If one assumes that the cross section of the emission cone is circular, then the duty cycles of pulsars suggest that the average beaming factor f is ~ 0.2. But Vivekanand and Narayan (1981) have argued that for short period pulsars, the emission cone may be highly elongated along the rotation axis, and the average beaming factor may be significantly larger. The local birthrate of pulsars estimated by Blaauw can be translated into the Galactic birthrate by scaling to the total area of the Galaxy. However, the concentration of pulsars is more in the inner

Galaxy than near the Sun. Using a correction factor to take into account this non-uniformity, one obtains a Galactic pulsar birthrate of one in ~25-50 yr corresponding to the beaming factor being in the range f = 0.2-0.4.

The Supernova Remnant (SNR) Birthrate

Several attempts have also been made to obtain the rate of formation of supernova remnants in our Galaxy. To do so, one assumes that all remnants with a surface brightness larger than that of an age calibrator are younger, or that all remnants smaller in size than that of a given calibrator are younger. If one can then estimate the age of the calibrator reliably, then this age t_c, divided by the total number of objects $N(<t_c)$ that are assumed to be younger than this remnant, gives the SNR birthrate τ:

$$\tau = t_c / N(<t_c).$$

The age estimate of a given remnant depends on the assumed evolutionary model. Clark and Caswell (1976) assumed that all SNRs have entered the decelerated "adiabatic" or "Sedov" phase of evolution, and obtained a birthrate of one in ~120 yr. This estimate must however be considered as a lower limit, since they assumed an interstellar density of ~1 atom/cc. There are strong reasons to believe that a certain fraction of the interstellar medium (ISM) consists of gas of much lower density. Lozinskaya (1979) and Higdon and Lingenfelter (1980) considered the effect of such a low density component of the ISM and, not surprisingly, obtained a much higher birthrate:

one in $\sim$30 yr. .

Srinivasan and Dwarakanath (1982) have argued that if the historical SNRs are typical, then their observed surface brightnesses suggest a much more rapid decline of surface brightness with age than would be predicted by the Sedov solution. Such a rapid rate of decline would yield smaller ages for the known remnants and hence a higher birthrate. Using such an approach they obtained a SNR birthrate of one in $\sim$20 yr.

We see, therefore, that within the errors the supernova rate, pulsar birthrate and SNR birthrate in the Galaxy agree reasonably well. In fig. 2.1 we have shown these three rates with the uncertainties indicated by the hatched regions. The marked scale gives the lower limit for the mass of the progenitors that these rates imply. However, though the present sample of supernova remnants in the Galaxy contains $\sim$150 objects, and the number of known pulsars exceed 400, only three cases of physical association between a pulsar and an SNR have been found (the Crab Nebula, the Vela SNR, and the SNR MSH 15-52).

This chapter is devoted to a discussion of the poor association between pulsars and SNRs.

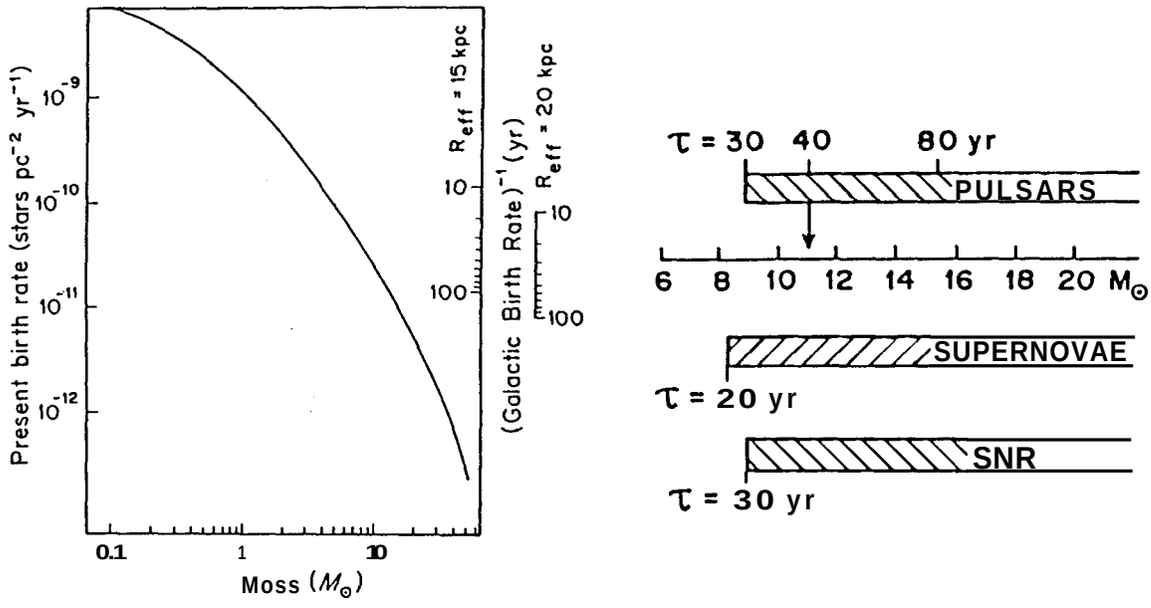

Fig. 2.1: (a) The integrated birthrate of stars in the local neighbourhood as derived by Miller and Scalo (1979). This can be used to derive the limiting mass of progenitors of pulsars, supernovae or supernova remnants given their Galactic birthrate and an effective radius for the Galaxy (this is different from the actual radius in order to account for the non-uniformity in the distribution of stars in the Galactic plane). This is indicated on the right.

(b) The lower limit for the mass of the progenitors implied by the pulsar birthrate, the frequency of supernovae and the birthrate of supernova remnants. The uncertainties in these rates are indicated by the hatched regions. R_{eff} = 20 kpc has been assumed.

The Standard Approach

The absence of pulsars in supernova remnants can, in principle, be rationalized by invoking several selection effects such as

a) Beaming

b) Pulse smearing due to interstellar electrons

c) Low radio fluxes of pulsars etc.

(Manchester and Taylor 1977). While the first factor permits only a fraction of such associations to be detected because the pulsar in many cases may not be beamed towards us, the second and the third factors severely restrict the detectability of pulsars beyond a distance of $\sim$2 kpc from the Sun. Most SNRs are situated at distances larger than this. Thus one doesn't expect to see many pulsars in SNRs.

But, as Radhakrishnan and Srinivasan (1980) have pointed out, even if absence of pulsars in SNRs may be accounted for this way, one should be able to detect the synchrotron nebulae (plerions) that such pulsars are expected to produce by pumping relativistic particles and magnetic field into the SNR cavity. The emission from the plerion, being isotropic and unpulsed, would not suffer from the first two selection effects 'mentioned above. Also, the radio luminosity of the plerion, as we shall see, will be very much larger than the radio luminosity of a typical pulsar, and the third selection effect is not likely to be serious. According to this

argument, if there is a pulsar in a supernova remnant, then its presence can be inferred by the centrally concentrated emission it will produce. This will result in a hybrid morphology for the remnant - a shell with a central concentration. In fact if the central pulsar is like the Crab pulsar, then the surface brightness of the central emission will be comparable or even greater than that of the shell component. But observations show that the overwhelming majority of SNRs have a shell morphology with hollow interiors. Faced with this difficulty Radhakrishnan and Srinivasan (1980) noted that shells with hollow interiors would be consistent with the presence of a central neutron star if for some reason it did not function as a pulsar, that is, it did not produce a strong relativistic wind with a frozen in magnetic field.

Such an extreme assumption may not however be necessary to explain the observed morphology of SNRs. In this chapter we explore the alternative that even though there may be a pulsar inside an SNR, for one or more reasons it is not able to produce a plerion of sufficient central brightness. In order to understand these reasons one has first to examine the theory of evolution of pulsar-produced nebulae. In the next section we review very briefly the theory due to Pacini and Salvati (1973) for the secular evolution of the radio luminosity of a plerion and isolate the most important and sensitive parameters.

In section 2.3 we estimate the lifetime of plerions as a function of the initial rotation period and magnetic field of the energising pulsar; this is done for two different models of nebular expansion. In section 2.3.3, we consider the case where the supernova ejecta is accelerated by the pressure of the relativistic wind from the pulsar, as we know to be the case for the Crab nebula. In section 2.3.4 we consider the alternative possibility that pulsars are born in rapidly expanding shells, the kinetic energy of the ejecta being derived from the original supernova blast wave. We find, in both cases, that to explain the rarity of plerions among the SNR sample, it is required that most pulsars are born either with long spin periods ($\gg$ 20 ms) or with rather low magnetic fields ($\ll 10^{12}$ Gauss), or both.

2.2 *EVOLUTION* OF PULSAR-PRODUCED NEBULAE

The evolution of the magnetic field, particle content and luminosity of an expanding nebula produced and maintained by a central pulsar has been discussed by Pacini and Salvati (1973) in their pioneering paper. We summarize below their approach and the main results. More details will be discussed in appendix 2.A2 to this chapter.

Input Physics And Formalism

The relativistic particles and magnetic fields responsible for the plerion emission are injected by the central pulsar at the expense of its rotational energy.

The rate of loss of rotational energy of the pulsar evolves with time as:

$$-\dot{E}_{rot} \equiv L_{PSR}(t) = \frac{L_o}{(1 + t/\tau_o)^{\alpha}} \qquad (2.1)$$

where L_o is the initial energy loss rate

τ_o is the initial spindown timescale, and

α is an exponent which is connected to the Braking index n as $\alpha = (n+1)/(n-1)$. (n is defined through the slowdown law $\dot{\Omega} \propto \Omega^n$; $\Omega(t)$ = angular frequency of rotation of the pulsar)

For a pure magnetic dipole radiator the braking index n should be equal to 3. Among the observed pulsars, the braking index has been measured for the Crab pulsar and PSR 1509-58, for which the values are 2.6 (Groth 1975) and 2.8 (Manchester, Durdin and Newton 1985) respectively.

One assumes that a fraction ϵ_p of the energy released is injected in the form of relativistic particles, and a fraction ϵ_m goes into the magnetic field of the nebula; $\epsilon_p + \epsilon_m \leq 1$. The injected energy spectrum of particles is assumed to be a flat power law upto a maximum energy E_{max}, i.e.,

$$J(E,t) = K(t) E^{-\gamma} \quad (E < E_{max} \; ; \; \gamma < 2) \qquad (2.2)$$

is the number of particles injected per unit time per unit energy interval. The exponent γ has a value of 1.6 for the Crab nebula. The normalisation factor $K(t)$ is obtained from

$$\int_0^{E_{max}} E\, J(E,t)\, dE = K(t) \int_0^{E_{max}} E^{1-\gamma} dE = \epsilon_p L_{PSR}(t). \quad (2.3)$$

The evolution of magnetic energy content is obtained using simple thermodynamics:

$$\frac{dW_B}{dt} + \frac{1}{3}\frac{W_B}{V}\frac{dV}{dt} = \epsilon_m L_{PSR}(t) \quad (2.4)$$

where $V(t)$ is the volume of the cavity and $W_B(t)$ is the magnetic energy content.

Since $W_B(t) = B^2 V/8\pi$, the solution of (2.4) yields the magnetic field $B(t)$ in the cavity.

Once the magnetic field is known, the evolution of energy $E(t)$ of an individual particle can be obtained from:

$$\frac{1}{ER} - \frac{1}{E_i R_i} = C_1 \int_{t_i}^{t} \frac{B^2(t)}{R(t)}\, dt \quad . \quad (2.5)$$

where E_i is the initial energy of the particle injected at time t_i. R_i and R are the radii of the cavity at times t_i and t respectively. Eq. (2.5) takes into account effects of both radiative and expansion losses of particle energy. C_1 is a constant related to the synchrotron radiation process.

The number of accumulated particles at an energy E at a time t is then obtained from:

$$N(E,t) = \int_0^t J(E_i, t_i) \frac{\partial E_i}{\partial E}\, dt_i \quad (2.6)$$

where E_i as a function of E, t and t_i is given by eq. (2.5).

Finally, the spectral luminosity $L_\nu(t)$ at a frequency ν at time t is calculated from the usual relation

$$L_\nu(t) = \frac{1}{2} c_1 \left(\frac{B\nu}{c_2^3}\right)^{1/2} N\left[\left(\frac{\nu}{c_2 B}\right)^{1/2}, t\right] \qquad (2.7)$$

where c_1 and c_2 are constants related to the synchrotron process.

Results

Pacini and Salvati isolated three major phases of evolution of a plerionic nebula:

1. The initial phase (phase I) lasts for a short period after the supernova explosion during which the expansion of the cavity is negligible. If v is the expansion velocity of the cavity and R_o its initial radius, then phase I refers to times $t \ll R_o / v$.

2. Phase II follows phase I and lasts till the initial spindown timescale τ_o of the central pulsar. For the Crab pulsar, the value of τ_o is $\sim$ 300 yr. During this phase the pulsar output L_{PSR} can be considered to be roughly constant at its initial value L_o. Most of the magnetic flux of the nebula is generated during this phase. As the nebula expands, the nebular luminosity, after an initial increase, slowly decreases with time.

3. At times $t > \tau_o$ the pulsar output decreases significantly. As the nebula continues to expand, the nebular luminosity decreases rapidly with time. This is referred to as Phase III.

Pacini and Salvati (1973) have presented expressions* for the time dependent spectral luminosity of a plerion at different frequency intervals. It can be seen from these expressions (also given in appendix 2.A2) that the spectral luminosity of a nebula at a given age depends on its expansion velocity, and the initial luminosity (L_o) and spindown timescale (τ_o) of the pulsar. These formulae can be rewritten in terms of the initial spin period and the magnetic field strength of the pulsar (appendix 2.A2). To illustrate a typical dependence of the plerion luminosity on these parameters, we reproduce below the expression for the radio spectral luminosity in phase III:

$$L_\nu(t) \propto B_*^{(3-5\eta)/2} P_o^{2(\eta-2)} \nu^{-3(1+\eta)/4} t^{-2\eta} \nu^{(1-\eta)/2} . \qquad (2.8)$$

In (2.8), B_* is the surface magnetic field of the pulsar, P_o its initial period and v the expansion velocity of the nebula. As was mentioned before, $\eta = 1.6$ for the Crab nebula, and if

---

* The treatment of Pacini and Salvati (1973) assumes a constant velocity of expansion for the plerion in all phases of its evolution. If, however, the pressure of the relativistic material causes significant acceleration of the expansion, as in the case of the Crab nebula, then their results are to be slightly modified. We have described these modifications in appendix 2.A1 and 2.A2. At late stages of evolution of the nebula interaction with the interstellar medium becomes important, and the expansion is decelerated. Evolution of plerions taking this deceleration into account will be discussed in chapter 5.

one uses this value, the above formula can be rewritten as

$$L_\nu \propto B_*^{-2.5} P_o^{-0.8} v^{-1.95} t^{-3.2} \nu^{-0.3}.$$

It can be seen from the above expression that the dependence of the spectral luminosity on the pulsar parameters and the velocity of expansion is quite strong. To understand the observed properties of the plerion population, one must therefore allow for a distribution in the initial parameters of the pulsars powering the nebulae, and also take into account different possible velocities of expansion. In the next section we shall attempt to obtain constraints on the distribution of pulsar parameters from the observed number 'of pulsar-produced nebulae and their luminosities.

2.3 LIFETIMES OF PLERIONS AND THEIR IMPLICATIONS

As we saw in the last section, the luminosity of a plerion depends on

- the period of the pulsar
- its magnetic field, and
- the expansion velocity of the boundary

Nebulae of the same age may have very different luminosities depending on these parameters. In what follows we shall assume that every pulsar produces a plerionic nebula. The detectability of such a nebula, however, will depend on its luminosity, which in turn will be determined by the magnetic

field and rotation period of the pulsar, as well as the expansion velocity of the nebula.

The time for which such a nebula will remain more luminous than a stipulated limit of detectability will be called the "**lifetime**" of the plerion. Clearly, the lifetime will be a function of the parameters mentioned above.

We shall now estimate the number of plerions one expects to see in the Galaxy above a certain luminosity limit, given a certain distribution of initial rotation periods and magnetic fields of pulsars. This can be obtained by multiplying the average lifetime by the birthrate of plerions. The birthrate of plerions is equal to the birthrate of pulsars, since every pulsar is assumed to produce a plerionic nebula. Therefore,

No. of plerions = (lifetime)x(pulsar birthrate),

This estimate of expected number of detectable plerions has to be made for different cases of expansion velocities. Finally, by comparing the expected number with the observed number of such plerions, we shall attempt to put constraints on the field-period distribution of pulsars at birth. For convenience this procedure is summarized in the Box below:

- Assume
  - an expansion velocity (or a model of expansion) of the SN ejecta
  - a pulsar birthrate
  - a distribution of the initial period and the magnetic fields.
- Estimate the number of plerions above a given luminosity limit.
- Compare with the observed number
- Change the assumed distribution of pulsar parameters till the predicted number is consistent with observations.

2.3.1 The Parameters Of The Pulsars

► Surface Magnetic Field

The distribution of the surface magnetic fields of pulsars, as derived from their observed periods and slowdown rates ($B \propto \sqrt{P\dot{P}}$), extends from 10^{11} G to $10^{13.5}$ G. However, there are reasons to believe that the distribution of pulsar fields at birth is much narrower (Radhakrishnan 1982). Pulsars with $B<10^{12}$ G are presumably several million years old, and consequently their fields would have decayed. If many pulsars are in fact born with fields less than 10^{12} G then it is very hard to understand why no pulsar has been found with a field less than that of the Crab, and with period less than $\sim$150 ms (see fig. 2.2). With such low fields, it will take

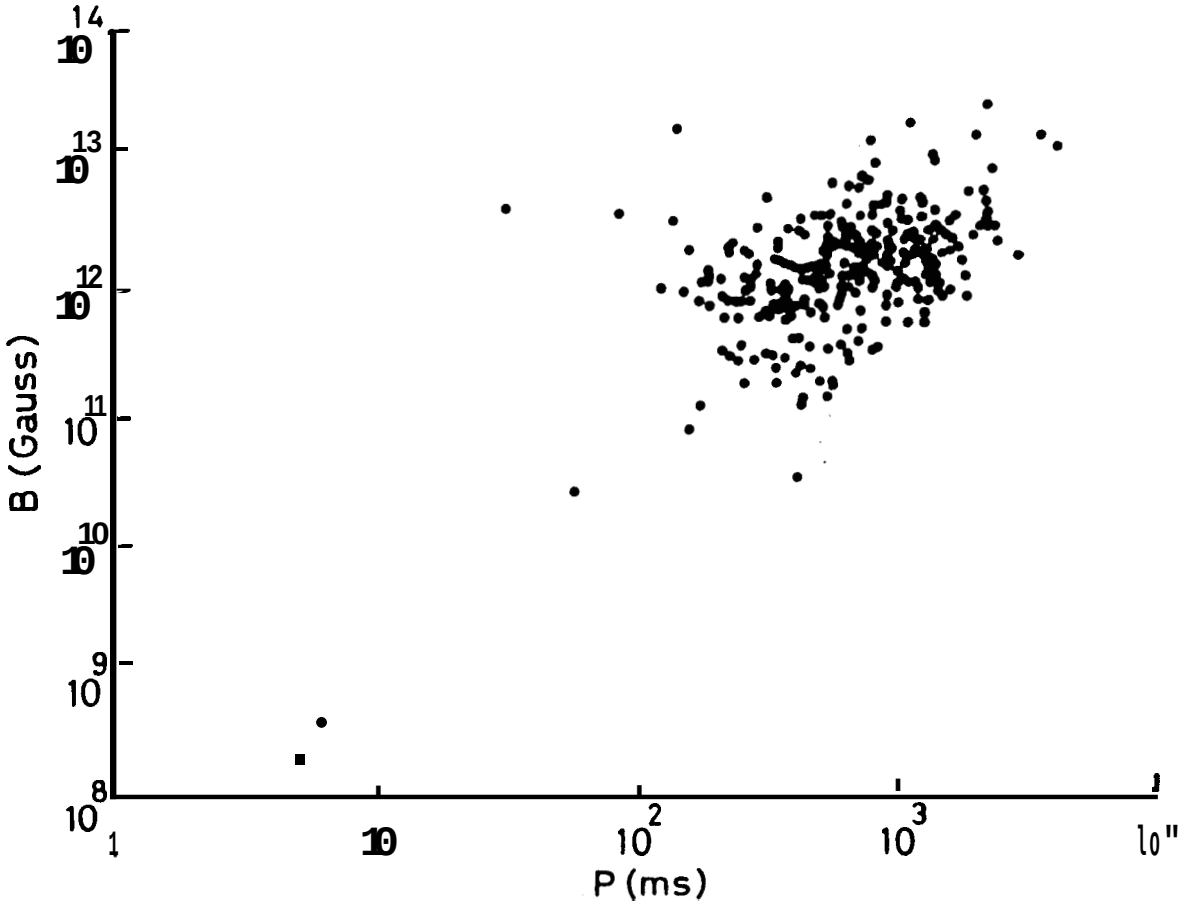

Fig. 2.2.: The distribution of rotation periods and derived magnetic fields of about 300 observed pulsars.

considerable time for their periods to lengthen to 150 ms, and consequently the chance of detection is significant. [The binary pulsar 1913+16 and the three recently discovered millisecond pulsars are believed to have low fields and short rotation periods due to their evolution in binary systems - see chapter 9; Radhakrishnan and Srinivasan (1982); van den Heuvel (1984); Radhakrishnan and Srinivasan (1984)]. Following Radhakrishnan (1982) we shall assume that the magnetic fields of pulsars at birth lie in the range 10^{12} - $10^{13.5}$ gauss. For simplicity we shall further assume that the distribution of magnetic fields in this interval is uniform in log B , i.e. the probability is equal for equal logarithmic intervals.

► Initial Spin Period

According to conventional belief, pulsars should be spinning with a period P ∼ a few milliseconds at birth. However, in the only case where we have a reliable estimate, namely for the Crab pulsar, the initial period was ∼16 ms. Therefore we shall, **to start with, allow the initial periods of pulsars to lie anywhere between 1 to 20 ms with equal probability.**

► Pulsar Birthrate

The estimate of expected number of plerions will require pulsar birthrate as an input. As mentioned before, estimated values of pulsar birthrate lie in the range of one in

$\sim$30-50 yr. For the sake of definiteness, we shall assume a pulsar birthrate of one in 40 yr.

2.3.2 Models For The Expansion Of The Nebular Boundary

In the standard model of a supernova, the envelope of the star is accelerated to a high velocity $\sim 10^4$ km/s by a shock wave. The kinetic energy of the ejecta is typically $\sim 10^{51}$ ergs. In type II explosions, the mass ejected is somewhat more than in a type I explosion, and therefore the velocities are correspondingly smaller. In section 2.3.4 we shall examine the consequences of an active pulsar in such a rapidly expanding cavity.

In the above scenario the pulsar does not have any dynamical role to play. One can envisage an alternative scenario in which it is the relativistic wind of a pulsar that accelerates the nebular boundary. The Crab nebula is an example of this scenario. It has been well established that the kinetic energy of expansion of the filamentary shell, as well as the acceleration experienced by it in the past, can be understood in terms of the energy being derived from the stored rotational energy of the newly born pulsar. The pressure of the relativistic "wind" from the pulsar and the magnetic field frozen into it accelerated it to the present velocity. Let $E_0 = I\Omega_0^2/2$ be the initial stored rotational energy of the pulsar. Here I is the moment of inertia of the neutron star and Ω_0 is the initial angular frequency of rotation. Within the initial characteristic slowdown time

$\tau_o = P_o / 2\dot{P}_o$, the pulsar would have released approximately half this energy in the form of relativistic particles and magnetic field. The kinetic energy of the ejecta will be a fraction of the energy thus released. If M_{ej} is the mass accelerated, then the velocity imparted to it by the pulsar can be estimated from

$$\frac{1}{2} M_{ej} v^2 \sim \frac{1}{2} E_o$$

$$\Rightarrow \quad v \propto \frac{1}{P_o M_{ej}^{1/2}}$$

if M_{ej} is roughly the same in all cases. Detailed dynamics of this acceleration process is described by Maceroni, Salvati and Pacini (1974), Reynolds and Chevalier (1984) and in appendix 2.A1. In the next subsection we shall discuss the evolution of plerion luminosity assuming that all plerions are pulsar-accelerated in the above manner.

2.3.3 Pulsar-driven Nebulae

The evolution of synchrotron nebulae whose boundaries have been accelerated by the pulsar have been discussed by Maceroni, Salvati and Pacini (1974), and Reynolds and Chevalier (1984). A detailed discussion of our working model is presented in appendix 2.A1 and 2.A2. In the initial phase, $t < \tau_o$, the velocity of expansion increases as $t^{1/2}$. After $t = \tau_o$ the pulsar energy output drops, and as a result acceleration becomes negligible. In this phase the nebula expands with a constant velocity $v \propto 1/(P_o M_{ej}^{1/2})$, till

deceleration sets in due to interaction with the interstellar medium. In what follows, however, we shall ignore the deceleration caused by the ISM interaction, so as to obtain more conservative limits on pulsar parameters, as will be clear from the following discussion. We shall assume that the mass ejected M_{ej} in all cases is roughly the same, and scale the expansion velocity in phase III ($t > \tau_o$) with respect to the Crab nebula, in inverse proportion to the initial rotation period:

$$v = 1700 \text{ km s}^{-1} (P_o/16\text{ms})^{-1}.$$

In fig. 2.3 we have compared the evolution of radio luminosity of different nebulae with central pulsars having different fields and initial periods. It can be seen from the figure that nebulae of the same age can have widely different luminosities depending upon the characteristics of the central pulsar. The same information is displayed in a more concise form in fig. 2.4. We have plotted contours of constant luminosity for a given age in the B_*-P_o plane. All pulsars with initial characteristics which lie on a given contour will produce nebulae of the same luminosity at a given age. In fig. 2.4a, the different contours correspond to different luminosities but the same age, whereas in fig. 2.4b, different contours correspond to different ages for the same luminosity.

One has now to set a **luminosity limit** such that if a nebula has a luminosity higher than that, it is unlikely to be missed anywhere in the Galaxy. The flux from the Crab nebula

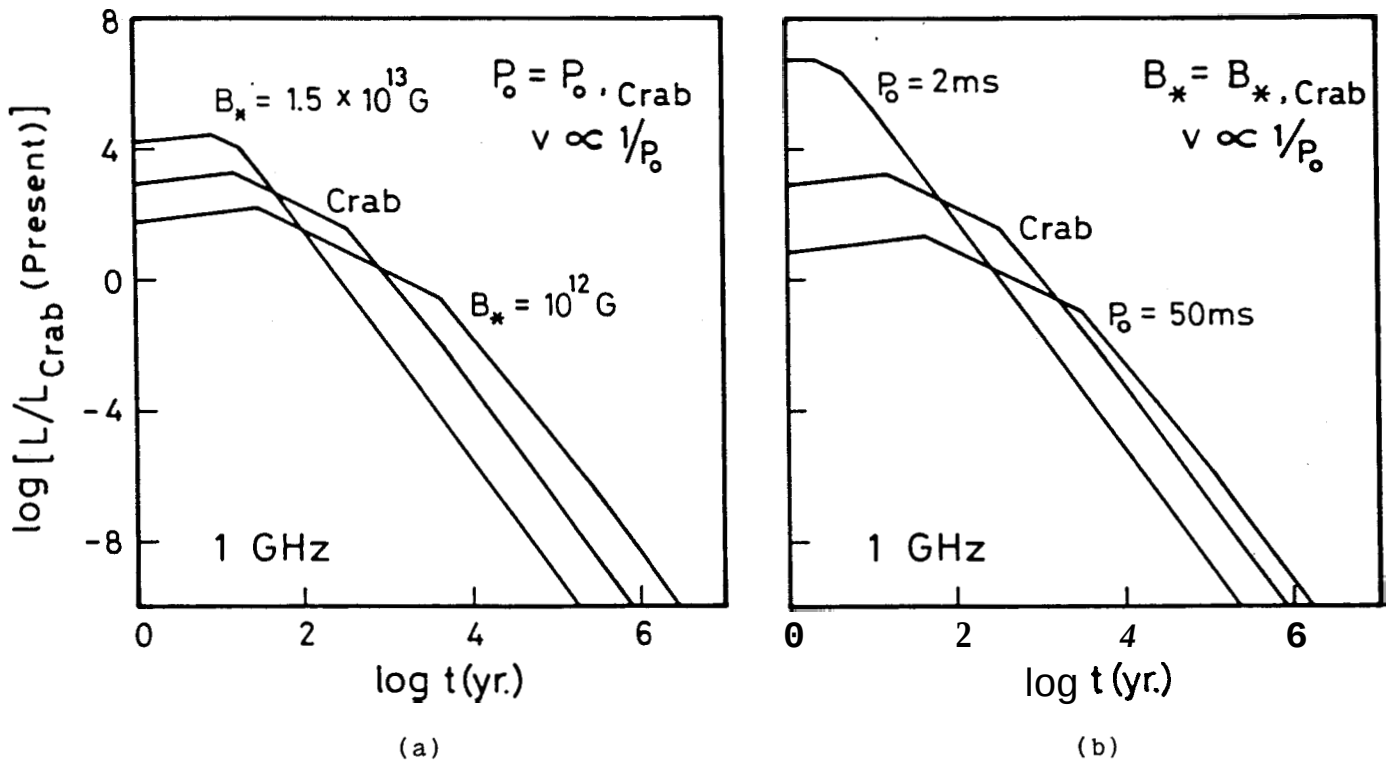

Fig. 2.3: The evolution of the radio spectral luminosity of pulsar-driven SNRs, in units of the present luminosity of the Crab nebula. (a) The evolutionary tracks of two such nebulae powered by pulsars with the same initial period as that of the Crab pulsar, but with different magnetic fields, are compared with the evolution of the Crab nebula. In (b), the pulsars are assumed to have the same magnetic field but different initial periods.

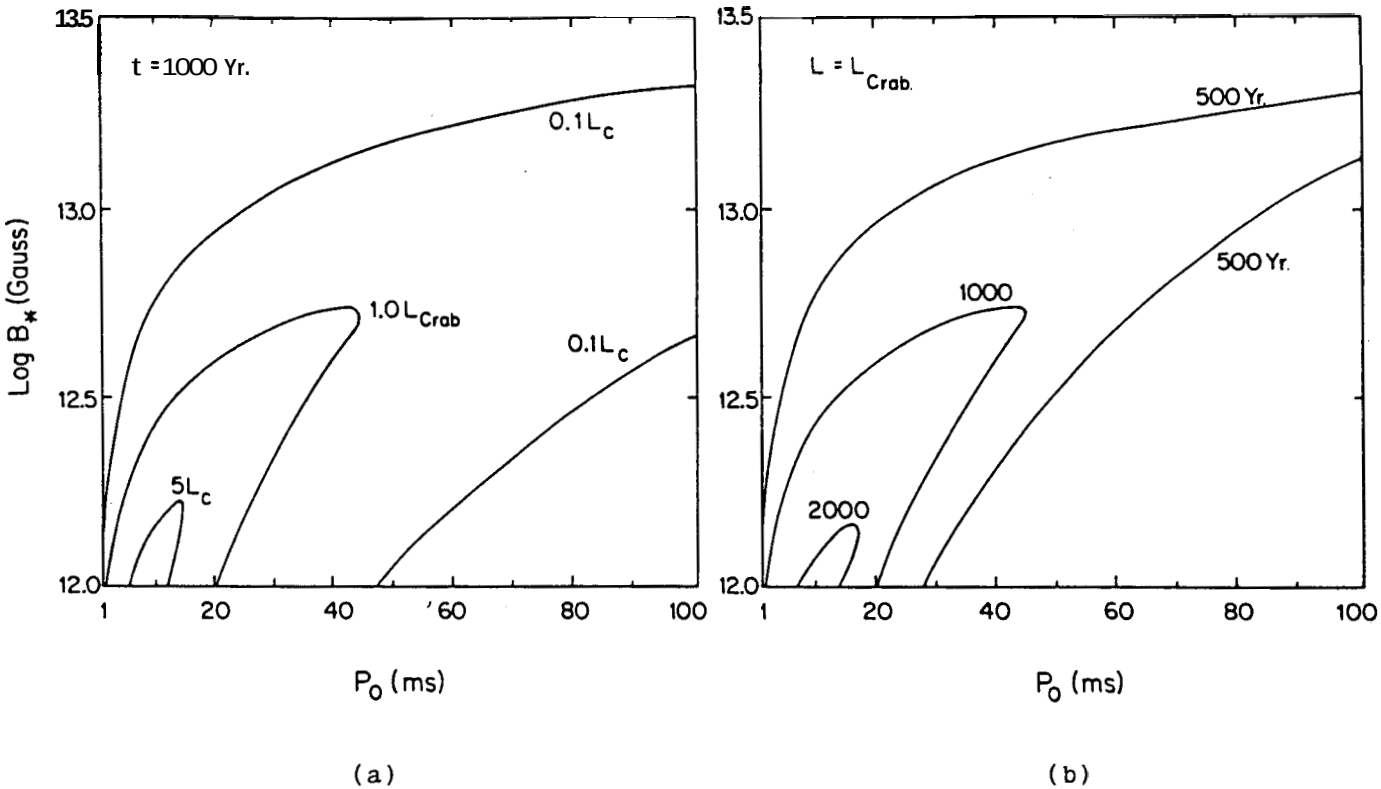

Fig. 2.4: Contours of constant luminosity of pulsar-driven nebulae are shown in the $B_* - P_o$ plane; here B_* is the surface magnetic field and P_o is the initial period of the pulsars. All pulsars born on a given contour will have the same luminosity at a specified age. (a) The three contours correspond to three different luminosities (measured in the units of the present luminosity of the Crab) and an age of 1000 yr. (b) The contours correspond to different ages, but the same luminosity, viz., the present luminosity of the Crab nebula.

will be 10 Jy at 1 GHz if placed at a distance of 20 kpc. The flux from a source with 1/10th the luminosity of the Crab will be 1 Jy at the same distance. It seems reasonable to suppose that many sources with flux greater than 1 Jy are unlikely to have been missed in surveys at frequencies around 1 GHz. It must be kept in mind that the plerions are likely to be more or less uniformly distributed in the inner Galaxy and that this flux limit corresponding to $L=0.1L_{Crab}$ refers to an extreme distance of 20 kpc. Therefore in what follows **we shall take $0.1L_{Crab}$ as the luminosity cut-off above which one should, in principle, be able to detect all sources in the Galaxy**. In fig. **2.5,** we have plotted several contours all corresponding to the above mentioned luminosity, namely $0.1L_{Crab}$. The labels on them represent the duration for which the nebulae are more luminous than the specified value, or in other words, their **lifetimes**. If is the mean interval between pulsar births, then the number N of nebulae that one expects to see above the threshold luminosity is given by

$$N(>) = \frac{1}{\tau} \int_0^\infty t\, f(t)\, dt \ . \qquad (2.9)$$

Here **f(t)dt** is the probability that a nebula will have a lifetime between t and **t+dt.** As we discussed above, the lifetime of the nebula depends on the initial parameters of the pulsar. The hatched area in the figure indicates the region where we assume the pulsars to be born with uniform probability.

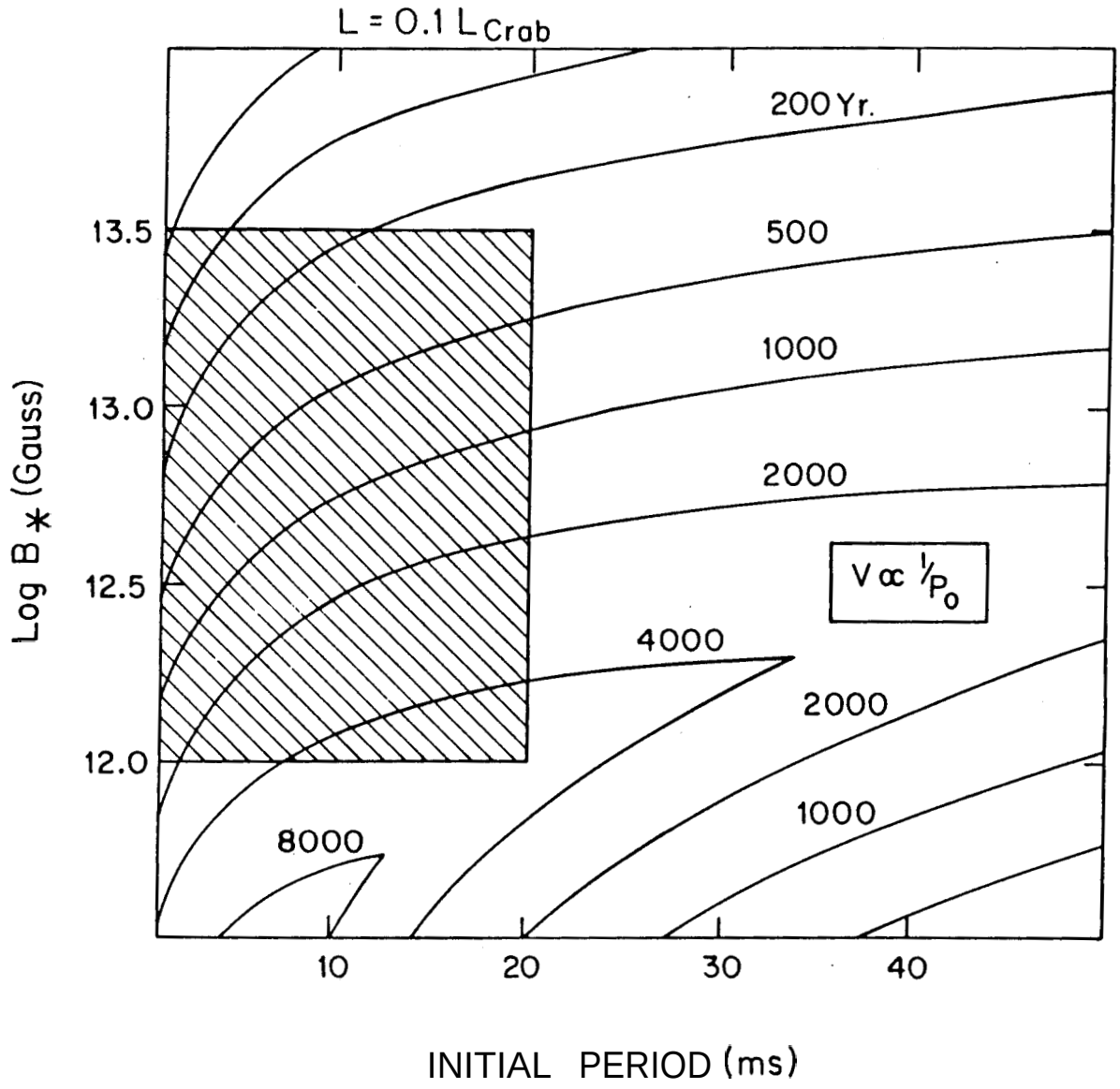

Fig. 2.5: Contours of different lifetimes above a luminosity limit of $0.1L_{Crab}$ for pulsar-driven nebulae. In estimating the expected number of plerions with luminosities greater than the above value, we have assumed that pulsars are born anywhere in the shaded region.

Table 2.1: Plerionic and Combination supernova remnants in our Galaxy

Source Name		Flux[b] (S) at 1GHz	Distance (d)	Luminosity[b] (Sd^2) at 1GHz	Type[a]	Ref.	Remarks
Galactic	Other	Jy	kpc	Jy-kpc^2			
G0.9+0.1		4.2(P) 8(S)	10?	420(P)? 800(S)?	C	1	
G6.5-0.1	W28	3(P) 330(S)	4	48(P) 5280(S)	C	2,3	
G20.2-0.2		10	4?	160?	P	3,4	
G21.5-0.9		7	5.5	212	P	3	
G24.7+0.6		20	?	?	P?	2	Possible plerion, but uncertain
G27.8+0.6		30	?	?	P?	2	Possible plerion, but uncertain
G29.7-0.3	Kes 75	0.4(P) 9.6(S)	7?	20(P)? 470(S)?	C	1,2,3	
G68.9+2.8	CTB 80	2(P) 100(S)	3	18(P) 900(S)	C?	2,3	Compact plerion-like core embedded in large steep spectrum arcs. No clear shell shape. Has been associated with SN of AD 1408

contd...

Table 2.1: Plerionic and Combination supernova remnants in our Galaxy (contd.)

Source Name		Flux[b] (S) at 1GHz	Distance (d)	Luminosity[b] (Sd^2) at 1GHz	Type[a]	Ref.	Remarks
Galactic	Other	Jy	kpc	Jy-kpc^2			
G74.9+1.2	CTB 87	8.6	12	1238	P	2,3	
G130.7+3.1	3C 58	33	2.6	223	P	2,3	Has been associated with SN of AD 1181
G184.6-5.8	Crab Nebula	1000	2	4000	P	2,3	Pulsar seen. Remnant of SN 1054 AD
G263.9-3.3	Vela XYZ	1100(P) 650(S)	0.5	275(P) 163(S)	C	2,3	Pulsar seen.
G291.0-0.1	MSH 11-62	16	?	?	P	3	
G320.4-1.2	MSH 15-52	70(S)	4.2	1235(S)	C	2,3	Pulsar seen. Plerionic component very weak in radio, but seen in X-rays.
G326.3-1.8	MSH 15-56	40(P) 100(S)	2[c]	160(P) 400(S)	C	2,5	

contd...

Table 2.1 : Plerionic and Combination supernova remnants in our Galaxy (contd.)

Source Name Galactic	Other	Flux[b] (S) at 1GHz Jy	Distance (d) kpc	Luminosity[b] (Sd^2) at 1GHz Jy-kpc^2	Type[a]	Ref.	Remarks
G327.4+0.4	Kes 27	33(S+P)	6?	1188(S+P)	C	2,6	Plerionic component not clearly seen in Radio, but X-rays have been detected.
G328.4+0.2	MSH 15-57	15	20?	6000?	P?	2	

Notes to Table 2.1:

[a] P stands for plerions and C for shell-plerion combination objects.

[b] In the case of combination remnants, P refers to the plerionic component and S to the shell component.

[c] Caswell et al (1975) give a distance of 1.5 kpc, although they do not rule out a larger distance of 4.6 kpc. They regard the latter estimate as unreliable without independent confirmation. The Σ-D relation for Galactic SNRs given by Mills (1983) yields a distance of ~2.2 kpc. Hence we assume a distance of ~2 kpc to this object.

References:

1. Helfand and Becker (1985)
2. Weiler (1983,1985)
3. Green (1987) and references therein
4. Becker and Helfand (1985)
5. Caswell et al (1 975)
6. Lamb and Markert (1981)

The integral in (2.9) is evaluated by calculating lifetimes on a 100 X 200 grid of log B vs P over the hatched portion of the diagram, and then computing the average. This yields the "average lifetime" of plerions. Multiplying this number by the pulsar birthrate ($\beta\ 1/\tau = (40yr)^{-1}$) one obtains the expected number N() of plerions above the stipulated luminosity limit.

We find that given the above distribution of the initial parameters of the pulsars, there should be ~37 nebulae whose luminosities are greater than 1/10th that of the Crab nebula, or in other words, whose fluxes would be greater than 1 Jy at 1 GHz even if placed at a distance of 20 kpc. However, from the list of known plerionic and combination remnants presented in table 2.1, it can be seen that there are at most three established plerionic nebulae with luminosities above $0.1L_{Crab}$. The newly discovered plerion G 0.9+0.1 may be an addition to the list if it is at a distance larger than 10 kpc (Helfand and Becker 1985). There is, of course, a remote possibility that the sample is grossly incomplete, but this is extremely unlikely in view of the fact that continued search with the VLA for such objects has so far yielded only one candidate (namely, G 0.9+0.1) which may have its luminosity above this value (Helfand et.al. 1984, Helfand and Becker 1985, Becker and Helfand 1985). The pulsar birthrate, which directly determines the expected number of plerions, could also be a source of error. It is, however, unlikely to be wrong by a factor of nine!

The only acceptable resolution seems to be that only a small fraction of pulsars are born inside the hatched region in fig. 2.5. There are three possibilities:

1. It may be that the majority of pulsars have fields larger than $10^{13.5}$ gauss. As can be seen from figs. 2.3 and 2.4 the plerions produced by such high field pulsars will be very shor -lived. But such high fields for the majority of pulsars is inconsistent with pulsar data (see fig. 2.2)

2. Alternatively, most pulsars have initial fields much less than 10^{12} gauss. These will not produce any bright plerions. But there is a difficulty with this alternative. The observed population of pulsars does not contain short period pulsars (P< 100 ms) with fields less than 10^{12} gauss. It is tempting to suggest that perhaps the radio luminosity of such low field pulsars may be small, but this is not consistent with the fact that one sees pulsars not only with such low fields, but also long periods (fig. 2.2). One can get out of this difficulty by saying that the magnetic fields of young neutron stars are so low that they do not function as pulsars at all. But in order to be consistent with the pulsar birthrate, their fields must grow to the canonical value in due course. The next chapter is devoted entirely to a discussion of this interesting possibility. It would be appropriate to mention now that the'conclusion we shall arrive at in chapter 3 is that even if the magnetic fields of pulsars are built after their birth, one 'cannot escape from

concluding that the most likely explanation is the following possibility:

3. The majority of pulsars are born spinning rather slowly, with initial periods longer than 20 milliseconds. In fact, for the predicted number of plerions to be consistent with the observed number, this "zone of avoidance" in the initial period must extend to about 150 ms, **i.e.,** the majority of pulsars must have their initial periods greater than this.

The Uniqueness *Of* The Crab Nebula

In the literature dealing with supernova remnants, the Crab nebula is often regarded as a "prototype". This stems from the fact that the Crab pulsar is regarded as a typical young pulsar. After all, it was conjectured even before pulsars were discovered that young neutron stars must be spinning very rapidly. The discovery of a rapid pulsar in the Crab nebula seemed to confirm this expectation. But this must be regarded as fortuitous because if each newly born pulsar is like the Crab pulsar, then they must all produce very bright nebulae. But there is only one Crab nebula in the **Galaxy!** Given the presently believed pulsar birthrate, this simple fact alone requires us to admit a wide distribution in initial periods and fields of pulsars.

A reference to figs. 2.3 and 2.4 shows that only when the pulsar's initial period lies in the range 10-20 milliseconds, and its field around 10^{12} -$10^{12.5}$ gauss, will the plerion be very bright, and long-lived. The uniqueness of the Crab nebula must be understood in terms of its pulsar having just these characteristics.

2.3.4 Pulsars Inside Rapidly Expanding Shells

As was mentioned before, according to the standard picture, the kinetic energy of expansion of the supernova ejecta is not derived from the stored rotational energy of the central pulsar but rather from a shock wave driven by the core bounce during the formation of the neutron star (Arnett, 1980). The velocity of the shell is determined by the strength of the shock wave and the mass in the envelope, and is expected to be $\sim$ 10,000 km s^{-1}. It is obvious that a pulsar in the centre of such a rapidly expanding shell will produce a much weaker plerion. We shall now estimate the number of plerions expected above our luminosity limit. At first sight it appears that even if all the pulsars are born spinning fast, one may not end up predicting too many plerions above our luminosity limit. But we shall see that this is not so.

Assuming the same range for the initial parameters of the pulsars as before (the hatched region in fig. 2.5), and also the same birthrate, we shall now estimate the number of plerions with luminosities greater than $0.1L_{crab}$ if the

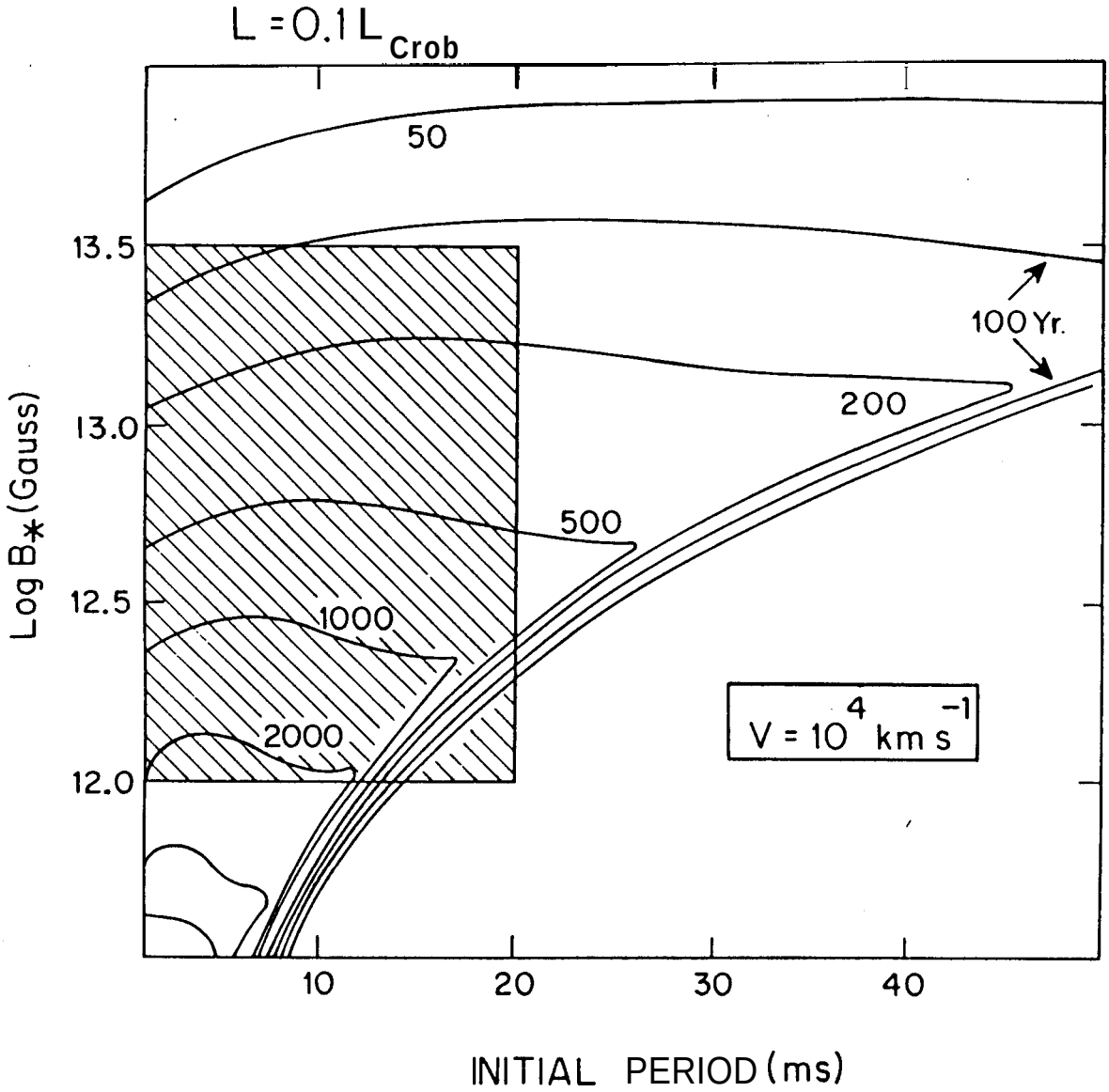

Fig. 2.6: Contours as in Fig. 2.5 for plerions produced by pulsars inside standard shell SNRs expanding with a velocity 10^4 km/s. The estimate of the expected number of such plerions has been carried out by allowing the initial parameters of pulsars to be distributed uniformly in the hatched region.

cavity is expanding with a velocity 10^4 km/s.

In fig. 2.6, we have plotted contours of different lifetimes corresponding to the luminosity limit mentioned above. Following the procedure outlined in detail in section 2.3.3, we arrive at the following *conclusion*. **There should be at least 15 plerions with luminosities greater than $0.1L_{crab}$ inside rapidly expanding shells.** This number will be even greater if the velocity of the shell is smaller than the assumed value of 10^4 km s^{-1} and/or if one takes into account the deceleration of the shell.

Although this number is less than the 37 predicted in the pulsar-driven scenario, the discrepancy with observations is even more glaring. From table 2.1 we see that there are only three centrally filled remnants above our luminosity limit. Of these, the Crab clearly does not belong to the scenario in discussion. This leaves G 328.4+0.2 and G 74.9+1.2. We shall now argue that **even** these two do not correspond to the present scenario of a pulsar inside a fast moving shock. When the shock sweeps up sufficient interstellar matter, one expects a pronounced radio and thermal X-ray shell. However, none of the three remnants mentioned above show any limb-brightening in the radio or an X-ray shell (Weiler, 1983; Becker, Helfand and Szymkowiak, 1982). One might argue that the radio shell is not pronounced because of very high central surface brightness due to the plerion. We shall return to this question in chapter 5. But one certainly expects to see an X-ray shell since the X-ray plerion will have a fairly small

spatial extent compared to the diameter of the shell. The newly discovered remnant, G 0.9-0.1, if situated at a distance larger than $\sim$10 kpc, may be the only example of a plerion with 1 GHz luminosity larger than $0.1L_{Crab}$, and with a shell around it.

If pulsars are not born in standard supernova explosions (type I or type II), then one could perhaps argue that the scenario under discussion is not a relevant one. But there is no reason to support such a "non-standard" birth for the majority of neutron stars. In fact, a pulsar has been detected inside a standard shell remnant (MSH 15-52).

Thus one is forced once again to the same conclusion as in the previous scenario, namely, that the initial periods of the majority of pulsars must be much greater than $\sim$20 ms.*

2.4 WHAT KIND OF PULSARS MAY BE PRESENT IN THE HISTORICAL SHELL SNRS?

According to the prevalent view historical shells such as Kepler, Tycho and SNR 1006 may be the remnants of Type I Supernovae which leave no compact remnants (Clark and Stephenson, 1977a; Trimble, 1983). Indeed, the absence of point thermal X-ray sources in them may be consistent with the above picture. In what follows, however, we shall assume that there are pulsars present and ask what kind of initial periods

---

*Strictly speaking, there are again three alternatives as mentioned in section 2.3.3, but for the reasons stated there we favour this conclusion.

Table 2.2: Historical shells considered

Source	Distance d kpc	Angular Diameter arcmin	Size pc	Age yr	Average Velocity of expansion km/s	$\frac{L_{plerion}}{L_{Crab}}$*	Ref.
SNR 185	2.5	39	28	1800	7800	<0.016	1,2
SNR 1006	1.3	34	12.8	980	6500	<0.002	1,3
RCW 103[a]	3.3	9.4	9	740	6000	<0.014	1,4
Kepler	3.5	3.2	3.3	380	4300	<0.012	1,5,6,7
Tycho	3	7.9	6.9	410	8400	<0.026	1,8,9,10

Notes to Table 2.2:

*Luminosity attributed to a possible central plerion

[a]This is not a Historical remnant. Nevertheless it is an important one for our discussion since a point X-ray source has been detected in it. We have estimated its age using the Σ-t relation given by Srinivasan and Dwarakanath (1982).

References:

1. Clark and Caswell (1976)
2. Caswell, Clark and Crawford (1975)
3. Milne (1971)
4. Caswell et al (1980)
5. Danziger and Goss (1980)
6. Gull (1975)
7. Matsui et al (1984)
8. Duin and Strom (1975)
9. Gorenstein, Seward and Tucker (1983)
10. Strom, Goss and Shaver (1982)

and fields they would have had? In none of these shells is there significant emission from the centre. From the published maps, one can get an actual estimate of the central emission only for the case of Kepler. The brightness temperature in the central region is less than 2 K, while the limb has an average brightness temperature $\sim$10 K. Central emission at such a low level is consistent with an optically thin shell whose thickness is, say, 1/5 the radius. But by attributing all of it to a possible central plerion, one can get an upper limit to its luminosity. From this we can put bounds on the parameters of a central pulsar. In the case of the other remnants, since no central emission is detected, one can get limits on the pulsar parameters by postulating a central plerion with a surface brightness 1/5th the average value for the remnant. Since we know the ages of these remnants, we can estimate their average expansion velocities. The fluxes and distances used are summarised in Table 2.2. In fig. 2.7, we have plotted for each of these remnants contours corresponding to Σ (plerion) = 1/5 Σ (average). The meaning of these contours is the following. Consider the one labelled "Kepler". If there is an active pulsar in its centre, then it could not have had an initial period and a field in the region enclosed by the contour. We have also included RCW 103, since there is a point X-ray source inside it. Its age was estimated to be 740 years using the Σ-t relation given by Srinivasan and Dwarakanath (1982). It should be remarked that for all the remnants except Kepler the limit on the excluded region for the pulsar is very weak, one has been generous in

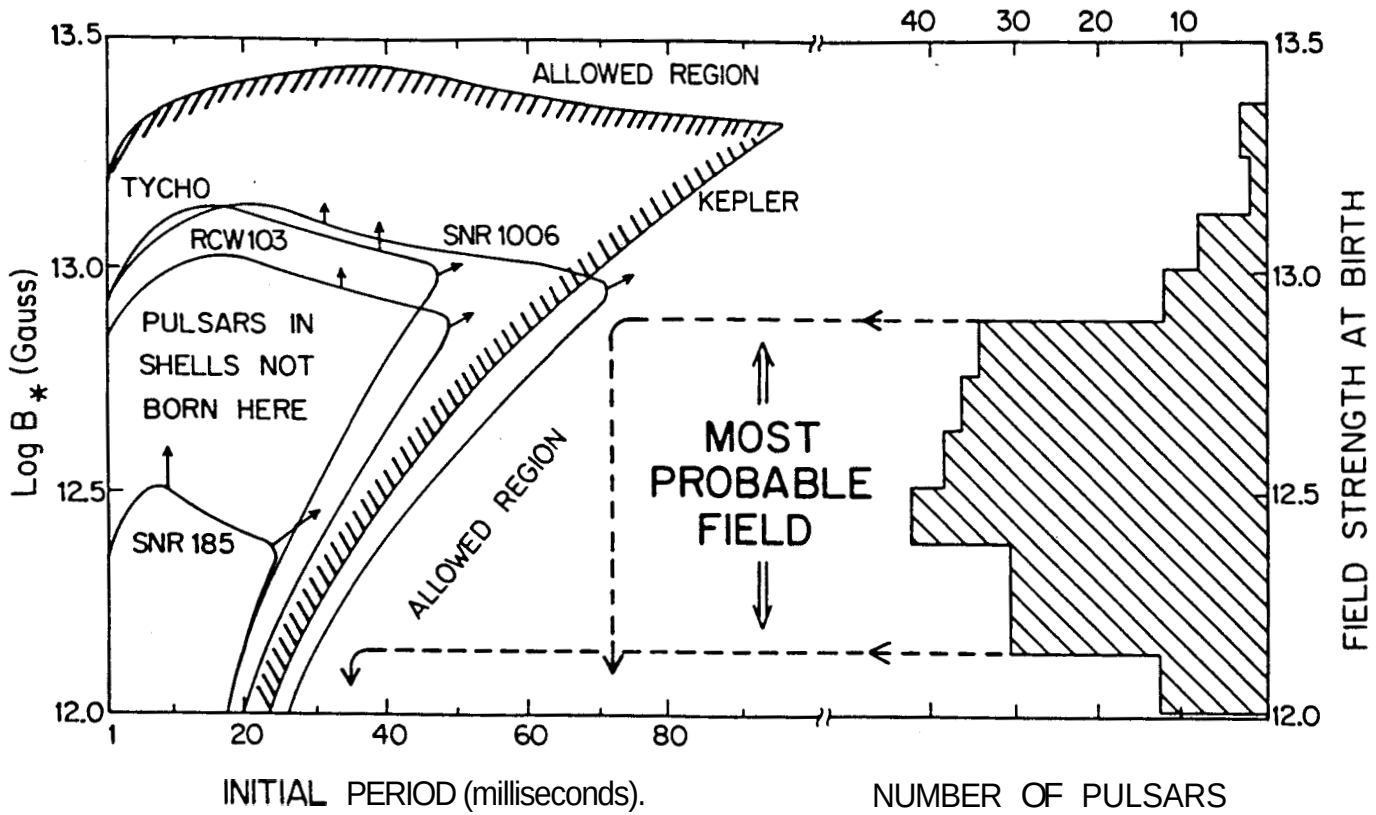

Fig. 2.7: Possible pulsars inside the Historical shell remnants. The contours correspond to surface brightness of an assumed central plerion equal to 1/5th the average surface brightness of the SNR; the appropriate ages and exqansion velocities inferred from their sizes were used. If pulsars in these shells were born inside the region enclosed by the contours, then the plerions produced by them should have been easily detected. The arrows on the contours indicate that the excluded region is likely to be much larger. Also shown is the histogram of pulsar fields at birth. Although pulsars in these remnants could have been born anywhere outside the region enclosed by the contours, the histogram suggests that the majority of them must be born with initial periods greater than 30-70 ms.

admitting a central plerion with as large a surface brightness as $1/5\,\Sigma(\text{average})$. A **more realistic value for the central surface brightness will increase the excluded region considerably,** bringing them closer to the contour for Kepler. We see from fig. 2.7 that if there are pulsars in these remnants, they must all have fields significantly greater than $10^{13.5}$ Gauss or lie to the right of the contours. Although one is dealing with a very small sample of historical **remnants,** it is striking that the conclusion is quantitatively similar in each case. Hence this may be statistically significant and suggest that pulsars in all the shells must have been born outside such an excluded region. In a prescient paper, Pacini (1972) arrived at the remarkable conclusion that the hollowness of the historical shells is consistent with the presence of very high field pulsars in them ($\gtrsim 10^{14}$ Gauss).

This may indeed be so in specific cases. But this cannot apply to the majority of shells for the following reason. In fig. 2.7 we have shown a histogram of the distribution of pulsar fields at birth. This has been derived from fig. 13 of Radhakrishnan (1982). It is seen that very few pulsars have fields greater than 10^{13} Gauss. This would imply that for the majority of pulsars in shells the period at birth must have been longer than 35-70 ms. We wish to regard this as a lower limit for the initial **periods** since the analysis was done not on the basis of measured fluxes from their centres, but on the basis of upper limits on them. Since the shell SNRs constitute more than 80% of the sample of SNRs, **the above**

conclusion applies to the majority of all pulsars. We shall return to the question of evolution of morphology and surface brightness of shell remnants containing pulsars in chapters 5 and 6.

2.5 RESULTS FROM PULSAR STATISTICS

An indication of slow initial rotation of pulsars was first obtained from a statistical analysis of pulsar data by Vivekanand and Narayan (1981). From the observed periods and period derivatives of pulsars, they were able to compute the average "current" of pulsars in different period-intervals. The current of pulsars J(P) is defined to be the number of pulsars crossing from periods shorter than P to longer than P per unit time. In a steady state, J(P) measures the birthrate minus deathrate of pulsars with period less than P. They found that the value of J(P) reaches a peak at periods > 0.7s, implying that many pulsars are born with such long periods. A more recent analysis of pulsar data by Narayan (1987), with more pulsars and incorporating all known selection effects against detectability of short-period pulsars, clearly shows this effect to be present.

A different statistical analysis, assuming dipole braking law for pulsars, has recently been performed by Chevalier and Emmering (1986). They, too, reached the conclusion that initial periods of pulsars must be larger than ~ 150 ms.

Our result is completely consistent with the above, and may be considered an independent confirmation of the same. It is interesting that independent analyses of pulsar and plerion statistics, from very different starting points, lead to similar conclusions.

2.6 CONCLUSIONS

The considerations that we have put forward in this chapter lead to the following conclusions:

1. If all plerions are like the Crab nebula, then given a pulsar birthrate of one in ~ 40 yr, one should see more than 35 radio plerions with luminosities greater than $\sim 0.1 L_{Crab}$, if their periods at birth are not more than 20 ms. There are only four plerions more luminous than this. This seems to suggest that either the majority of pulsars are born spinning slowly ($P_o > 150$ ms), or that pulsar-driven supernova remnants are extremely rare.

2. The Crab nebula must be a very rare object even among pulsar-driven plerions. Only in the rare case when the initial period of the pulsar is ~ 20 ms and its magnetic field $\sim 10^{12}$ gauss will the plerion be as bright and as long-lived as the Crab nebula. The particular nature of the Crab nebula should be understood in terms of the Crab pulsar having just these characteristics.

3. If the energy of expansion of the plerion is not derived from the stored rotational energy of the pulsar, then it must come from the supernova shock wave. In this case, one expects the nebular boundary to be expanding with a velocity $\sim 10^4$ km/s. One expects to see more than 15 SNRs with hybrid morphology with the central radio plerion more luminous than 0.1 L_{Crab} if all pulsars are born spinning as rapidly as the Crab pulsar or faster. Among the known combination remnants, at most one fits this description. From this, we conclude that pulsars inside shell SNRs must have initial periods substantially larger than that of the Crab pulsar.

4. We have estimated the characteristics of pulsars in the historical shells from (generous) limits on the surface brightness of associated plerions (fig. 2.7). In all cases, the bounds are similar, forcing us to the conclusion that pulsars in shell SNRs are born with periods greater than 35-70 ms. This provides strong support for the conclusion arrived at by Vivekanand and Narayan (1981) from an analysis of the periods and period derivatives of pulsars that the majority of them make their "appearence" with periods >100 ms.

Very recently, pulsar surveys have been conducted with improved sensitivity for detection of short period pulsars (Stokes et.al. 1986; Clifton and Lyne 1986). The results show beyond doubt a distinct deficit of pulsars with periods less

than $\sim$ 100 milliseconds. According to Stokes **et.al. (1986),** the high luminosities of Crab and Vela - like pulsars would allow them to be seen throughout a substantial portion of the Galaxy. In the volume of the Galaxy surveyed by them, normal pulsars with periods less than $\sim$100 milliseconds comprise at most 1% or so of the population of active pulsars. The only viable explanation of this deficit is that pulsars are born with rotation periods longer than 100 milliseconds.

The conclusion that spin periods of pulsars at birth should be not a few milliseconds, but a few hundred milliseconds has thus been reached in three independent ways - analysis of pulsar statistics **(Vivekanand** and Narayan 1981; Narayan **1987),** from paucity of bright plerions (above; Srinivasan, Bhattacharya and Dwarakanath **1984)** and from the results of newly conducted pulsar surveys. This certainly strengthens the result and leaves little room for an alternative.

APPENDIX 2.A1

Expansion of a pulsar-driven nebula

The expansion of supernova ejecta under the dynamical influence of a pulsar has been discussed by Ostriker and Gunn (1971); Maceroni, Salvati and Pacini (1974) and Reynolds and Chevalier (1984). We describe here the behaviour of a simple model following these authors.

We assume that the nebula consists of the following three components.

(i) An expanding thin spherical shell of supernova ejecta of total mass M. This shell has a radius $R(t)$ and forms the boundary of the nebula. The mass swept up from the ambient medium is neglected.

(ii) A mixture of relativistic particles and magnetic field in the cavity bounded by the shell. The pressure of this relativistic fluid is responsible for the expansion of the shell. We shall consider this pressure to be the only force acting on the shell*.

(iii) A central pulsar which continuously generates the relativistic material and deposits it into the nebula.

---

* This assumption is valid in the intermediate age of the nebula. At later stages of evolution the mass swept up from the interstellar medium would modify the dynamics, and in the very early stages the gravitational attraction of the central neutron star may play an important role (see Maceroni, Salvati and Pacini (1974) for a detailed discussion).

Under these conditions, the equation of motion of the shell can be written as:

$$M_{ej} \frac{d^2R}{dt^2} = 4\pi R^2 p_{rel} \qquad (2.A1.1)$$

where $p_{rel}(t)$ is the pressure of the relativistic fluid.

The above pressure p_{rel} can be obtained from simple thermodynamics:

$$\frac{dU_{rel}}{dt} + p_{rel} \frac{dV}{dt} = L - \Lambda \qquad (2.A1.2)$$

where $U_{rel}(t)$ is the total energy of the relativistic fluid in the cavity, $V(t)$ is the volume of the cavity, $L(t)$ is the rate of deposition of energy by the pulsar and $\Lambda(t)$ is the radiative luminosity of the nebula.

In the following we shall assume that all the energy injected in the form of relativistic particles is lost in radiation* . Thus in (2.A1.2) the quantity at the right hand side equals the rate of deposition of energy in the cavity in the form of magnetic field.

Assuming that the slowdown law of the pulsar is of the form

$$-\dot{\Omega} \propto \Omega^n ,$$

---

* This assumption is justified in view of the flat energy spectrum of particles in pulsar produced nebulae. In such energy distributions, major contribution to the total energy comes from the high energy end, where radiation losses of the particle energies are severe.

one gets a spindown luminosity for the pulsar

$$L(t) = \frac{L_0}{(1 + t/\tau_0)^{\alpha}} \qquad (2.A1.3)$$

where =(I . For a pure dipole model n =3 and α =2. τ_0 is called the initial spindown timescale of the pulsar.

If a fraction ϵ_m of this energy goes into the magnetic field then, as mentioned above,

$$L(t) - \Lambda(t) = \epsilon_m L_0 / (1 + t/\tau_0)^{\alpha}. \qquad (2.A1.4)$$

We shall consider two asymptotic limits of (2.A1.4):

$$\underline{t << \tau_0}: \qquad L - \Lambda = \epsilon_m L_0 \quad . \qquad (2.A1.5)$$

$$\underline{t >> \tau_0}: \qquad L - \Lambda = \epsilon_m L_0 \left(t/\tau_0\right)^{-\alpha}. \qquad (2.A1.6)$$

Using the relations

$$p_{rel}(t) = \frac{1}{3} \frac{U_{rel}(t)}{V(t)} \; ; \; V(t) = \frac{4\pi}{3} R^3(t) \qquad (2.A1.7)$$

we can now rewrite (2.A1.2) as

$$\frac{d}{dt}\left(p_{rel} R^4\right) = (L - \Lambda) R \quad . \qquad (2.A1.8)$$

Combining (2.A1.1) and (2.A1.8) one gets

$$M_{ej}\left(2\dot{R}\ddot{R} + R\dddot{R}\right) = L - \Lambda \qquad (2.A1.9)$$

where dot denotes the time derivative.
Integrating with the boundary condition $R(t=0) = 0$,

$$M_{ej}\left(\frac{1}{2}\dot{R}^2 + R\ddot{R}\right) = \int_0^t (L-\Lambda)\,dt \qquad (2.A1.10)$$

at $t \ll \tau$, (2.A1.5) and (2.A1.10) give

$$M_{ej}\left(\frac{1}{2}\dot{R}^2 + R\ddot{R}\right) = \epsilon_m L_o t . \qquad (2.A1.11)$$

(2.A1.11) has a solution

$$R(t) = \left(\frac{8\epsilon_m L_o}{15 M_{ej}}\right)^{1/2} t^{3/2} . \qquad (2.A1.12)$$

This is the expansion law for the nebula in the early phase, $(t \ll \tau_o)$, when the pulsar output is roughly constant. At $t \gg \tau_o$ the pulsar output drops substantially and the acceleration becomes negligible. The shell coasts with an uniform velocity

$$v \sim \dot{R}(\tau_o) . \qquad (2.A1.13)$$

If we define a velocity v through

$$v \equiv \frac{3}{2}\left(\frac{8\epsilon_m L_o}{15 M_{ej}}\right)^{1/2} \tau_o^{1/2} \qquad (2.A1.14)$$

then the expansion of the nebula is well approximated by the piecewise continuous expressions

$$\boxed{R(t) = (v/\tau_o^{1/2})\, t^{3/2} \quad \text{for } t<\tau_o} \qquad (2.A1.15)$$

&

$$\boxed{R(t) = vt \quad \text{for } t>\tau_o}. \qquad (2.A1.16)$$

In our models of pulsar-driven supernova remnants we have adopted the expansion laws obtained above.

In the dipole model of the pulsar, $L_o \propto B_*^2/P_o^4$, and $\tau_o \propto P_o^2/B_*^2$; where B_* is the magnetic field of the pulsar and P_o its initial rotation period. From (2.A1.14) we then find that the terminal velocity of the nebula is proportional to $(L_o\tau_o)^{1/2} \propto \frac{1}{P_a}$.

APPENDIX 2.A2

Spectral evolution of a pulsar produced nebula

Spectral evolution of a uniformly expanding plerion has been discussed by Pacini and Salvati (1973). In this appendix we briefly review their work, and then discuss the modifications necessary to allow for the accelerated expansion in the early phase of a pulsar-driven nebula.

The relativistic particles and the magnetic field in a plerion come at the expense of the rotational energy of the pulsar. The pulsar loses energy at a rate

$$-\dot{E}_{rot} \equiv L_{PSR}(t) = \frac{L_o}{(1 + t/\tau_o)^{\alpha}} \qquad (2.A2.1)$$

where τ_o is the initial spindown timescale of the pulsar. The exponent α takes a value equal to 2 for a pure dipole model. The measured values of α are 2.3 for the Crab pulsar and 2.1 for PSR 1509-58. In our models we assume α =2.3.

A fraction ϵ_m of this energy is injected in the form of magnetic fields and a fraction ϵ_p in the form of particles; $\epsilon_m + \epsilon_p \leq 1$. In our models we have adopted the values = $_p$ =0.5, as did Pacini and Salvati (1973).

Pacini and Salvati (1973) identified three distinct phases in the evolution of the nebula:

Phase I: In this initial phase the nebula has not expanded much beyond the original size of the envelope. The adiabatic losses of the particle and the field energies are negligible, and during this phase the magnetic field of the nebula reaches its peak. This phase, however, lasts for a very short time and so we shall not discuss this phase in detail.

Phase II: This phase follows phase I and lasts till $t = \tau_o$. The pulsar luminosity L_{PSR} can be considered roughly constant during this phase:

$$L_{PSR} = L_o \qquad (2.A2.2)$$

(small t limit of 2.A2.1).

Phase III: This phase corresponds to times $t > \tau_o$. In this phase the luminosity of the pulsar is approximated by the expression

$$L_{PSR} = L_o \left(t/\tau_o\right)^{-\alpha} \qquad (2.A2.3)$$

(large t limit of 2.A2.1)

We shall first consider the case of uniform expansion of the nebula with a velocity v.

2.A2.1 Evolution Of Magnetic Field

The evolution of nebular magnetic field can be calculated from the thermodynamic relation

$$\frac{dW_B}{dt} + \frac{W_B}{3V}\frac{dV}{dt} = \epsilon_m L_{PSR} \qquad (2.A2.4)$$

where W_B is the magnetic energy content of the nebula and V is its volume. $W_B/3V$ gives the magnetic pressure. Using $V = \frac{4\pi}{3} R^3$, (2.A2.4) can be rewritten as

$$\frac{d}{dt}(RW_B) = \epsilon_m L_{PSR} R$$

or,

$$W_B(t) = \frac{1}{R(t)} \int_0^t \epsilon_m L_{PSR}(t') R(t') dt'.$$

Writing $W_B = \frac{B^2}{8\pi} V = \frac{1}{6} B^2 R^3$, where B is the nebular magnetic field, we find

$$B^2(t) = \frac{6}{R^4(t)} \int_0^t \epsilon_m L_{PSR}(t') R(t') dt'. \qquad (2.A2.5)$$

We shall use this expression to evaluate the nebular magnetic field in the different phases. Since we are considering a case of uniform expansion, and also times much beyond phase I, we may write $R(t) = vt$, and (2.A2.5) reduces to

$$B^2(t) = \frac{6\epsilon_m}{v^3 t^4} \int_0^t L_{PSR}(t') \cdot t' \cdot dt' \qquad (2.A2.6)$$

where ϵ_m has been assumed to be independent of time.

Phase II

In phase II $L_{PSR}(t) = L_0$; and

$$B^2(t) = \frac{3\epsilon_m L_0}{v^3 t^2}$$

i.e. $$\boxed{B(t) = \left(\frac{3\epsilon_m L_0}{v^3}\right)^{1/2} t^{-1}} \quad . \qquad (2.A2.7)$$

It should be noted that although the magnetic field B decreases with time, the magnetic flux ($\propto BR^2$) increases. Thus. most of the magnetic flux of the nebula is generated during this phase.

Please turn over

Phase III

The magnetic field in phase III can be obtained from

$$B^2(t) = \frac{6\epsilon_m}{v^3 t^4}\left[\int_0^{\tau_0} L_0 t' dt' + \int_{\tau_0}^{t} L_0 \left(\frac{t'}{\tau_0}\right)^{-\alpha} t' dt'\right]$$

$$= \frac{3\alpha\epsilon_m L_0 \tau_0^2}{(\alpha-2)v^3 t^4}\left[1 - \frac{2}{\alpha}\left(\frac{t}{\tau_0}\right)^{2-\alpha}\right]$$

$$\simeq \frac{3\alpha\epsilon_m L_0 \tau_0^2}{(\alpha-2)v^3 t^4} \quad \text{for } t \gg \tau_0 \text{ and } \alpha > 2 .$$

i.e.
$$\boxed{B(t) \simeq \left[\frac{3\alpha\epsilon_m L_0 \tau_0^2}{(\alpha-2)v^3}\right]^{1/2} t^{-2}} . \qquad (2.A2.8)$$

It can be seen that since most of the magnetic flux is generated in phase II, the magnetic field evolves as R^{-2} in phase III, typical of expansion with conserved flux.

2.A2.2 Particle Energy Distribution

Having found the behaviour of the field, we now need to know the number of relativistic particles as a function of energy to calculate the synchrotron luminosity of the nebula.

The pulsar is assumed to iniect a power law spectrum of particles upto a maximum energy E_{max}. We write

$$J(E,t) = K(t)\,E^{-\gamma} \quad (E \leq E_{max}) \qquad (2.A2.9)$$

as the number of particles injected per unit time per unit energy interval around E at time t. The energy index γ is found to be less than 2 in all pulsar-produced nebulae. The coefficient $K(t)$ is obtained from the normalization condition

$$\int_0^{E_{max}} E\,J(E,t)\,dE = \epsilon_p L_{PSR}(t)\,. \qquad (2.A2.10)$$

Once injected, the energy of a particle changes with time due to synchrotron and adiabatic losses. The evolution of particle energy is governed by the equation

$$-\frac{dE}{dt} = c_1 B^2 E^2 + \frac{\dot{R}}{R} E \qquad (2.A2.11)$$

where the first term in the right hand side corresponds to radiation loss, and the second term gives the adiabatic loss rate. $c_1 = 2.37 \times 10^{-3}$ erg^{-1}s^{-1} gauss^{-2} is a constant connected with the Synchrotron process *.

It is clear from 2.A2.11 that the particles with low energies mainly undergo expansion losses, while for particles with high energies synchrotron losses are dominant. The dividing line between these two regimes is called the "break energy" E_b, defined through

---

* We assume that the distribution of pitch angle of particles are isotropic around the local direction of the magnetic field at any point.

$$c_1 B^2 E_b^2 = \frac{\dot{R}}{R} E_b$$

$$\text{or,} \qquad E_b = \frac{1}{c_1 B^2 (R/\dot{R})}$$

With $R(t)=vt$, we can write

$$E_b = \frac{1}{c_1 B^2 t} . \qquad (2.A2.12)$$

We shall treat the particles with $E > E_b$ and $E < E_b$ separately, and consider only radiation losses for the former and adiabatic losses for the latter. Strictly speaking, there will be a class of particles for which synchrotron losses are important in the beginning, but later they lose energy mainly due to expansion. However, it can be shown that such particles do not make a significant contribution to the particle distribution except for a small region near E_b. We shall therefore ignore the presence of particles with such intermediate energies.

The energy E at a time t of a particle that was injected with energy E_i at time t_i can then be obtained from:

Please turn over'

$$E = E_i \frac{t_i}{t} \quad \text{for } E < E_b \qquad (2.A2.13)$$

and

$$\frac{1}{E} - \frac{1}{E_i} = C_1 \int_{t_i}^{t} B^2 dt \quad \text{for } E > E_b. \qquad (2.A2.14)$$

Once the relation between E, t and E_i, t_i are established, the energy distribution of the accumulated particles is determined from

$$N(E,t) = \int_{E}^{E_{max}} J\left[E_i, t_i(t, E, E_i)\right] \frac{\partial t_i}{\partial E} dE_i$$

.....(2.A2.15a)

or equivalently from

$$N(E,t) = \int_{0}^{t} J\left[E_i(E, t, t_i), t_i\right] \frac{\partial E_i}{\partial E} dt_i .$$

.....(2.A2.15b)

We shall now determine the particle energy distribution in different phases of evolution of the nebula.

Phase II

From (2.A2.10) and (2.A2.2), the coefficient $K(t)$ of the injection rate is found to be

$$K(t) = (2-\gamma)\, \epsilon_p L_o E_{max}^{\gamma-2} . \qquad (2.A2.16)$$

The break energy E_b evolves as

$$E_b = \frac{1}{c_1 B^2 t} = \frac{v^3 t}{3 c_1 \epsilon_m L_0} \cdot \qquad (2.A2.17)$$

For $E < E_b$, (2.A2.13) gives

$$t_i = t \frac{E}{E_i} \quad ,$$

i.e.

$$\frac{\partial t_i}{\partial E} = \frac{t}{E_i}$$

and hence

$$N(E,t) = (2-\gamma) \epsilon_p L_0 E_{max}^{\gamma-2} t \int_E^{E_*} E_i^{-\gamma-1} d E_i$$

where E_* is the maximum energy of the particles at injection which make appearance at energy E at time t, having undergone only adiabatic losses. Since $\gamma > 0$, the lower limit of the integration dominates and we find

$$N(E,t) = \frac{(2-\gamma) \epsilon_p L_0 E_{max}^{\gamma-2} t}{\gamma} E^{-\gamma} \qquad (2.A2.18)$$

$$(E < E_b)$$

on the other hand, for $E > E_b$,

$$\frac{1}{E} - \frac{1}{E_i} = \frac{3 \epsilon_m L_0 c_1}{v^3} \left(\frac{1}{t_i} - \frac{1}{t} \right)$$

which gives $$\frac{\partial t_i}{\partial E} = \frac{v^3 t_i^2}{3\epsilon_m L_o c_1 E^2}$$

for $E \gg E_b$, $t_i \approx t$, and

$$\frac{\partial t_i}{\partial E} \approx \frac{v^3 t^2}{3\epsilon_m L_o c_1 E^2} .$$

Using this in (2.A2.15), we find

$$N(E,t) = \frac{(2-\gamma)\epsilon_p L_o E_{max}^{\gamma-2} v^3 t^2}{3\epsilon_m L_o c_1 E^2} \int_E^{E_{max}} E_i^{-\gamma} dE_i .$$

As $\gamma > 1$, the lower limit dominates, and we find

$$N(E,t) \simeq \frac{(2-\gamma)\epsilon_p E_{max}^{\gamma-2} v^3 t^2}{3(\gamma-1)\epsilon_m c_1} E^{-(\gamma+1)} \qquad (E > E_b). \qquad \text{(2.A2.19)}$$

Phase III

In phase III, $K(t)$ is given by

$$K(t) = (2-\gamma)\epsilon_p L_o E_{max}^{\gamma-2} \left(\frac{t}{\tau_o}\right)^{-\alpha} . \qquad \text{(2.A2.20)}$$

The break energy evolves as

$$E_b = \frac{1}{c_1 B^2 t} = \frac{(\alpha-2) v^3 t^3}{3\alpha \epsilon_m c_1 L_o \tau_o^2} . \qquad \text{(2.A2.21)}$$

At $E < E_b$, the particle distribution will consist of two kinds of particles: (1) the old particles, which were injected in phase II; and (2) the fresh particles injected in phase III.

Let $E_b(\tau_o)$ be the break energy at $t=\tau_o$. The number of particles with energies higher than $E_b(\tau_o)$ at $t=\tau_o$ is so small that they do not make any significant contribution to the particle distribution in phase III. So we shall ignore these particles in the old population. The particle spectrum below $E_b(\tau_o)$ at $t=\tau_o$ was, from (2.A2.18),

$$N_o(E,\tau_o) = \frac{(2-\gamma)\epsilon_p L_o E_{max}^{\gamma-2}\tau_o}{\gamma} E^{-\gamma}.$$

These particles suffer adiabatic losses in phase III and are found below the energy

$$E_c(t) \equiv E_b(\tau_o)\frac{\tau_o}{t} = \frac{v^3\tau_o}{3c_1\epsilon_m L_o t}. \quad (2.A2.22)$$

Below this energy, the spectrum of the old particles at time t would be

$$N(E,t) = N_o(E_\tau,\tau_o)\frac{dE_\tau}{dt}$$

where $E_\tau = E\frac{t}{\tau_o}$ is the energy a particle with energy E at time t would have had at time τ_o. Thus, the relic particle spectrum at time $t>\tau_o$ is described by

$$N(E,t) = \frac{(2-\gamma)\epsilon_p L_o E_{max}^{\gamma-2}}{\gamma}\tau_o^{\gamma} t^{1-\gamma} E^{-\gamma} \quad (2.A2.23)$$

$$(E<E_c).$$

Now, the spectrum of fresh particles in this energy interval

is obtained as follows:

Since particles suffer only adiabatic losses,

$$E_i = E\frac{t}{t_i} \quad \text{and} \quad \frac{\partial E_i}{\partial E} = \frac{t}{t_i} \ .$$

Then, from (2.A2.15) and (2.A2.20)

$$N(E,t) = (2-\gamma)\epsilon_p L_0 E_{max}^{\gamma-2} t^{1-\gamma} E^{-\gamma} \tau_0^{\alpha} \int_{\tau_0}^{t} t_i^{\gamma-\alpha-1}\, dt_i \ .$$

Since $\alpha > \gamma$, the lower limit dominates, and we get

$$N(E,t) = \frac{2-\gamma}{\alpha-\gamma}\epsilon_p L_0 E_{max}^{\gamma-2} \tau_0^{\gamma} t^{1-\gamma} E^{-\gamma} \ . \qquad (2.A2.24)$$

Therefore, within our approximations the old particles (2.A2.23) and the fresh particles (2.A2.24) make almost equal contribution, and their spectra are identical.

At energies $E > E_b(t)$ given by (2.A2.21), all particles suffer radiation losses and

$$\frac{1}{E} - \frac{1}{E_i} = \frac{3\alpha\epsilon_m L_0 \tau_0^2}{(\alpha-2)v^3} \cdot \frac{1}{3}\left[\frac{1}{t_i^3} - \frac{1}{t^3}\right]$$

giving $t_i \simeq t$, and

$$\frac{\partial t_i}{\partial E} = \frac{(\alpha-2)v^3}{3\alpha\epsilon_m c_1 L_0 \tau_0^2} \cdot \frac{t_i^4}{E^2} \simeq \frac{(\alpha-2)v^3}{3\alpha\epsilon_m c_1 L_0 \tau_0^2} \cdot \frac{t^4}{E^2}$$

thus

$$N(E,t) = \frac{(\alpha-2)(2-\gamma)\epsilon_p E_{max}^{\gamma-2} \tau_o^{\alpha-2} v^3 t^4}{3\epsilon_m \alpha c_1} t^{-\alpha} \int_E^{E_{max}} E_i^{-\gamma} dE_i .$$

As $\gamma > 1$, the lower limit dominates, and

$$N(E,t) = \frac{(\alpha-2)(2-\gamma)\epsilon_p E_{max}^{\gamma-2} v^3 \tau_o^{\alpha-2} t^{4-\alpha}}{3(\gamma-1)\epsilon_m \alpha c_1} E^{-(\gamma+1)} \quad (2.A2.25)$$

$$(E > E_b) .$$

Between E_b and E_c there'are two kinds of fresh particles:

(i) Those which have always suffered adiabatic losses - these particles would have been injected with an energy $E_i < E_*$; $E_* \equiv \left[\frac{(\alpha-2) v^3 E^3 t^3}{3\alpha c_1 \epsilon_m L_o \tau_o^2}\right]^{1/4}$, and

(ii) Those which have first suffered synchrotron losses, and then adiabatic losses. They would have been injected with energy between E_* and E_{max} . However, it can be shown that the particles of the first category dominate the spectrum, and hence the spectrum of particles in this energy interval is given by

$$N(E,t) = (2-\gamma)\epsilon_p L_o E_{max}^{\gamma-2} \tau_o^{\alpha} t^{1-\alpha} E^{-\alpha} \int_E^{E_*} E_i^{\alpha-\gamma-1} dE_i$$

since $\alpha > \gamma$, the upper limit dominates, i.e.

$$N(E,t) = \frac{2-\gamma}{\alpha-\gamma}\left[\frac{\alpha-2}{3\alpha\epsilon_m c_1}\right]^{(\alpha-\gamma)/4} \epsilon_p^{(4-\alpha+\gamma)/4} L_0 E_{max}^{\gamma-2} \times v^{3(\alpha-\gamma)/4} \tau_0^{(\alpha+\gamma)/2} t^{(4-\alpha-3\gamma)/4} E^{-(\alpha+3\gamma)/4}$$

$$(E_c < E < E_b). \qquad \text{.....(2.A2.26)}$$

As the break energy E_b continues to increase, it will at some time t_* reach the maximum injected energy E_{max}. At $t > t_*$, the evolution of all particles are fully adiabatic, and at energies $E > \bar{E} = E_{max}\frac{t_*}{t}$ the absence of injection above $E = E_{max}$ modifies the spectrum. In the range $\bar{E} < E < E_{max}$, the particle spectrum is given by

$$N(E,t) = (2-\gamma)\epsilon_p L_0 E_{max}^{\gamma-2} \tau_0^{\alpha} t^{1-\alpha} E^{-\alpha} \int_E^{E_{max}} E_i^{\alpha-\gamma-1} dE_i .$$

The upper limit contributes, and we get

$$N(E,t) = \frac{2-\gamma}{\alpha-\gamma}\epsilon_p L_0 E_{max}^{\alpha-2} \tau_0^{\alpha} t^{1-\alpha} E^{-\alpha} \qquad \text{(2.A2.27)}$$

$$(\bar{E} < E < E_{max}).$$

At energies below $\bar{E}$, (2.A2.26) still holds.

However, if the time t_* at which E_b crosses E_{max} is reached before $t = \tau_0$, i.e. in phase II, then the evolution of particle spectrum in phase III is fully adiabatic, and contains only two distinct sections. Below $\tilde{E} = E_{max}\frac{\tau}{t}$,

the spectrum is given by (2.A2.24) and above $\tilde{E}$ by (2.A2.27).

2.A2.3 Radiation Spectrum

Once the particle distribution and the magnetic field in the nebula are known, the radiation spectrum can be computed from

$$L_\nu(t) = \frac{1}{2} C_1 \left(\frac{B\nu}{C_2^3}\right)^{1/2} N\left[\left(\frac{\nu}{C_2 B}\right)^{1/2}, t\right] \qquad (2.A2.28)$$

which results from the so-called "monochromatic approximation", namely that an electron of energy E radiates its entire synchrotron power at a frequency $\nu = C_2 B E^2$. This gives more than adequate accuracy for our purpose.

We summarize below the spectral luminosities obtained using (2.A2.28) and the expressions for particle distribution and magnetic fields derived above.

Phase II

At a frequency $\nu < \nu_b \equiv c_2 B E_b^2$

$$L_\nu(t) = \frac{2-q}{2q} c_1 c_2^{(q-3)/2} \epsilon_p (3\epsilon_m)^{(1+q)/4} L_0^{(q+5)/4} E_{max}^{q-2} \times \nu^{-3(1+q)/4} t^{(1-q)/2} \nu^{(1-q)/2}$$

.....(2.A2.29)

and at a frequency $\nu > \nu_b$

$$L_\nu(t) = \frac{1}{2} \cdot 3^{(q-2)/4} \cdot \frac{2-q}{q-1} c_2^{(q-2)/2} \epsilon_p \epsilon_m^{(q-2)/4} E_{max}^{q-2} \times \nu^{3(2-q)/4} L_0^{(q+2)/4} t^{1-\frac{q}{2}} \nu^{-q/2}.$$

.....(2.A2.30)

Phase III

$$L_\nu(t) = \frac{1}{2} C_1 C_2^{(\eta-3)/2} \left[\frac{3\alpha\epsilon_m}{\alpha-2}\right]^{(1+\eta)/4} \epsilon_p^{\frac{\alpha(2-\eta)}{-\eta-(\alpha-\eta)}} E_{max}^{\eta-2}$$

$$\times L_o^{(\eta+5)/4} \tau_o^{(3\eta+1)/2} \vartheta^{-3(\eta+1)/4}$$

$$\times t^{-2\eta} \nu^{(1-\eta)/2}$$

$$\text{for} \quad \nu < \nu_c \equiv \nu_b(\tau_o)\,(\tau_o/t)^4$$

.....(2.A2.31)

$$L_\nu(t) = \frac{1}{2}\frac{2-\eta}{\alpha-\eta}\left(\frac{3\alpha\epsilon_m}{\alpha-2}\right)^{(4-\alpha-7\eta)/16} C_1^{(4+\eta-\alpha)/4} C_2^{(\alpha+3\eta-12)/8}$$

$$\times \epsilon_p E_{max}^{\eta-2} L_o^{(7\eta-3\alpha+20)/16} \vartheta^{-\frac{3}{16}(7\eta-3\alpha+4)}$$

$$\times \tau_o^{(7\eta+5\alpha+4)/8} t^{-(\alpha+3\eta)/2}$$

$$\times \nu^{(4-\alpha-3\eta)/8}$$

$$\text{for} \quad \nu_c < \nu < \nu_b$$

.....(2.A2.32)

and

$$L_\nu(t) = \frac{1}{2}\,\frac{2-\eta}{\eta-1}\left(\frac{\alpha-2}{3\alpha\epsilon_m}\right)^{\frac{2-\eta}{4}} \epsilon_p\, C_2^{(\eta-2)/2}\, E_{max}^{\eta-2} \times L_0^{(\eta+2)/4}\, \vartheta^{-\frac{3}{4}(\eta-2)}\, \tau_0^{(\eta+2\alpha-2)/2} \times t^{2-\alpha-\eta}\, \nu^{-\eta/2}$$

$$\text{for } \nu > \nu_b \ . \qquad \text{.....(2.A2.33)}$$

At $t > t_*$, the spectrum at a frequency $\nu > \bar{\nu} \equiv c_2 B \bar{E}^2$ is given by

$$L_\nu(t) = \frac{1}{2}\cdot\frac{2-\eta}{\alpha-\eta}\left(\frac{3\alpha\epsilon_m}{\alpha-2}\right)^{(1+\alpha)/4} \epsilon_p\, c_1\, c_2^{(\alpha-3)/2} \times L_0^{(\alpha+5)/4}\, \vartheta^{-\frac{3}{4}(\alpha+1)}\, \tau_0^{(1+3\alpha)/2}\, E_{max}^{\alpha-2} \times t^{-2\alpha}\, \nu^{(1-\alpha)/2} \ .$$

.....(2.A2.34)

If $E_b(\tau_0) \geq E_{max}$, the radiation spectrum in phase III contains only two segments, given by (2.A2.31) for $\nu < \tilde{\nu} \equiv c_2 B E_{max}^2 \left(\frac{\tau_0}{t}\right)^2$, and by (2.A2.34) for $\nu > \tilde{\nu}$.

2.A2.4 Accelereted Expansion

We shall now incorporate the acceleration of the expansion in phase II for a pulsar-driven nebula. According

to the dynamical results derived in appendix 2.A1, we can write the nebular radius as a function of time as

$$R = v \tau_0^{-1/2} t^{3/2} \qquad \text{in phase II}$$

and $R = vt$ in phase III

where $v = \frac{3}{2}\left(\frac{8\epsilon_m L_0 \tau_0}{15 M_{ej}}\right)^{1/2}$, M_{ej} being the mass in the ejecta.

In phase III, since $R(t)$ has the same form as in the case of a uniformly expanding nebula, no modification is necessary in the expressions for magnetic field, particle distribution and spectral luminosity as long as the velocity given by the above expression is used to evaluate them. But the expressions for phase II need modification. The magnetic field in phase II is obtained by rewriting (2.A2.5) as

$$B^2(t) = \frac{6\tau_0^{3/2}}{v^3 t^6} \epsilon_m L_0 \int_0^t t'^{3/2} dt'$$

which yields

$$B(t) = \left(\frac{12}{5} \frac{\epsilon_m L_0}{v^3}\right)^{1/2} \tau_0^{3/4} t^{-7/4}. \qquad (2.A2.35)$$

The break energy E_b in this case is given by

$$E_b = \frac{1}{c_1 B^2 (R/\dot{R})} = \frac{3}{2 c_1 B^2 t}$$

$$= \frac{5 v^3 t^{5/2}}{8 \epsilon_m c_1 L_o \tau_o^{3/2}} \quad . \qquad (2.A2.36)$$

At $E < E_b$, particles suffer only adiabatic losses, and their energies evolve as

$$E^2 t^3 = E_i^2 t_i^3 \quad .$$

Therefore $t_i = t \left(\frac{E}{E_i}\right)^{2/3}$, and $\frac{\partial t_i}{\partial E} = \frac{2}{3} \frac{t}{(E E_i)^{1/3}}$.
Using these, and (2.A2.15), one finds

$$N(E,t) = \frac{2(2-\gamma)}{3\gamma - 1} \epsilon_p E_{max}^{\gamma-2} L_o t E^{-\gamma} \qquad (2.A2.37)$$

for $E < E_b$.

At $E > E_b$

$$\frac{1}{E} - \frac{1}{E_i} = \frac{2}{5} c_1 \cdot \frac{12}{5} \frac{\epsilon_m L_o}{v^3} \tau_o^{3/2} \left[t_i^{-5/2} - t^{-5/2} \right]$$

which yields

$$t_i \simeq t, \quad \text{and} \quad \frac{\partial t_i}{\partial E} \simeq \frac{5 v^3 t^{7/2}}{12 c_1 \epsilon_m L_o \tau_o^{3/2} E^2}$$

Using these, we find

$$N(E,t) = \frac{5}{12}\,\frac{2-\gamma}{\gamma-1}\,\frac{\epsilon_b}{c_1\epsilon_m}\,E_{max}^{\gamma-2}\,\tau_o^{-3/2}\,\vartheta^3\,t^{7/2}\,E^{-(\gamma+1)}$$

$$\text{for} \quad E > E_b \,. \qquad \text{.....(2.A2.38)}$$

Radiation spectrum in phase II can now be calculated using the above expressions for magnetic field and particle spectrum. We list below the results.

$$L_\nu(t) = \frac{2-\gamma}{3\gamma-1}\left(\frac{12\epsilon_m}{5}\right)^{\frac{1+\gamma}{4}}\epsilon_b\,c_1 c_2^{(\gamma-3)/2}\,E_{max}^{\gamma-2}$$
$$\times\, L_o^{(\gamma+5)/4}\,\vartheta^{-3(1+\gamma)/4}\,\tau_o^{3(1+\gamma)/8}$$
$$\times\, t^{(1-7\gamma)/8}\,\nu^{(1-\gamma)/2}$$

$$\text{for} \quad \nu < \nu_b \qquad \text{.....(2.A2.39)}$$

and

$$L_\nu(t) = \frac{1}{2} \cdot \frac{2-\gamma}{\gamma-1} \cdot \left(\frac{12\,\epsilon_m}{5}\right)^{\frac{\gamma-2}{4}} \epsilon_p\, C_2^{(\gamma-2)/2}\, E_{max}^{\gamma-2} \times L_0^{(2+\gamma)/4}\, \tau_0^{3(\gamma-2)/8}\, v^{3(\gamma-2)/4}\, t^{7(2-\gamma)/8} \times \nu^{-\gamma/2}$$

$$\text{for } \nu > \nu_b \,. \qquad \ldots\ldots(2.A2.40)$$

2.A2.5 Dependence Of Spectral Luminosity On Pulsar Parameters: Scaling Laws

The expressions for spectral luminosities obtained above can be rewritten in terms of the magnetic field B_* and initial rotation period P_0 of the central pulsar, using the following dependences.

$$L_0 \propto B_*^2 / P_0^4$$

$$\tau_0 \propto P_0^2 / B_*^2$$

and in the case of pulsar-accelerated nebula, the terminal velocity

$$v \propto 1/P_0$$ (see appendix **2.A1**).

We summarize below the scaling relations thus obtained.

Phase II

A. Uniform expansion:

$$L_\nu(t) \propto B_*^{(\eta+5)/2} P_o^{-(\eta+5)} \vartheta^{-\frac{3}{4}(\eta+1)} t^{(1-\eta)/2} \times \nu^{(1-\eta)/2}$$

$$(\nu < \nu_b)$$

.....(2.A2.41)

and

$$L_\nu(t) \propto B_*^{(\eta+2)/2} P_o^{-(\eta+2)} \vartheta^{\frac{3}{4}(2-\eta)} t^{1-\frac{\eta}{2}} \nu^{-\eta/2}$$

$$(\nu > \nu_b).$$

.....(2.A2.42)

B. Accelerated expansion:

$$L_\nu(t) \propto B_*^{(7-\eta)/4} P_o^{(\eta-7)/2} t^{(1-7\eta)/8} \nu^{(1-\eta)/2}$$

$$(\nu < \nu_b)$$

.....(2.A2.43)

and

$$L_\nu(t) \propto B_*^{(10-\gamma)/4} P_o^{(\gamma-10)/2} t^{\frac{7}{8}(2-\gamma)} \nu^{-\gamma/2}$$

$$(\nu > \nu_b).$$

.....(2.A2.44)

Phase III

A. No acceleration in phase II

$$L_\nu(t) \propto B_*^{(3-5\gamma)/2} P_o^{2(\gamma-2)} v^{-\frac{3}{4}(1+\gamma)} t^{-2\gamma} \nu^{(1-\gamma)/2}$$

$$(\nu < \nu_c)$$

.....(2.A2.45)

$$L_\nu(t) \propto B_*^{(12-7\gamma-13\alpha)/8} P_o^{2(\alpha-2)} v^{-\frac{3}{16}(7\gamma-3\alpha+4)} \times t^{-(\alpha+3\gamma)/2} \nu^{(4-\alpha-3\gamma)/8}$$

$$(\nu_c < \nu < \nu_b \text{ or } \bar{\nu})$$

.....(2.A2.46)

$$L_\nu(t) \propto B_*^{(6-\gamma-4\alpha)/2} P_o^{2(\alpha-2)} \vartheta^{-\frac{3}{4}(\gamma-2)} \times t^{2-\alpha-\gamma} \nu^{-\gamma/2}$$

$$(\nu > \nu_b ; t < t_*)$$

.....(2.A2.47)

and

$$L_\nu(t) \propto B_*^{(3-5\alpha)/2} P_o^{2(\alpha-2)} \vartheta^{-\frac{3}{4}(\alpha+1)} t^{-2\alpha} \times \nu^{(1-\alpha)/2}$$

$$(\nu > \bar{\nu} ; t > t_*).$$

.....(2.A2.48)

B. With acceleration in phase II

In this case the terminal velocity ϑ of the nebula is determined by P_o, and the above relations can be rewritten as

$$L_\nu(t) \propto B_*^{(3-5\gamma)/2} P_o^{(11\gamma-13)/4} t^{-2\gamma} \nu^{(1-\gamma)/2}$$

$$(\nu < \nu_c)$$

.....(2.A2.49)

$$L_\nu(t) \propto B_*^{(12-7\eta-13\alpha)/8} P_o^{(21\eta+23\alpha-52)/16} \times t^{-(\alpha+3\eta)/2} \nu^{(4-\alpha-3\eta)/8}$$

$$(\nu_c < \nu < \nu_b \text{ or } \bar{\nu})$$

.....(2.A2.50)

$$L_\nu(t) \propto B_*^{(6-\eta-4\alpha)/2} P_o^{(3\eta+8\alpha-22)/4} \times t^{2-\alpha-\eta} \nu^{-\eta/2}$$

$$(\nu > \nu_b;\ t < t_*)$$

.....(2.A2.51)

and

$$L_\nu(t) \propto B_*^{(3-5\alpha)/2} P_o^{(11\alpha-13)/4} t^{-2\alpha} \nu^{(1-\alpha)/2}$$

$$(\nu > \bar{\nu};\ t > t_*).$$

.....(2.A2.52)

REFERENCES

Arnett, W.D., 1980, Ann. N. Y. Acad. Sci., 336, 366-379

Baade, W., Zwicky, F., 1934, Phys. Rev'., 45, 138

Becker, R.H., Helfand, D.J., 1985, Astrophys. J., 297, L25-L28

Becker, R.H., Helfand, D.J., Szymkowiak, A.E., 1982, Astrophys. J., 255, 557-563

Blaauw, A., 1985, in: Birth and Evolution of Massive Stars and Stellar Groups, eds. Boland, W., van Woerden, H., D. Reidel, Dordrecht, p.211-224

Blaauw, A., 1987, in IAU Symp. no. 125: Origin and Evolution of Neutron Stars, eds. D.J. Helfand and J.H. Huang, D. Reidel, Dordrecht, in press

Caswell, J.L., Clark, D.H., Crawford, D.F., 1975, Aust. J. Phys. Astrophys. Suppl. no. 37, 39-56

Caswell, J.L., Haynes, R.F., Milne, D.K., Wellington, K.J., 1980, Mon. Not. R. astr. Soc., 190, 881-889

Caswell, J.L., Murray, J.D., Roger, R.S., Cole, D.J., Cooke, D.J., 1975, Astr. Astrophys., 45, 239-258

Chevalier, R.A., Emmering, R.T., 1986, Astrophys. J., 304, 140-153

Clark, D.H., Caswell, J.L., 1976, Mon. Not. R. astr. Soc., 174, 267-305

Clark, D.H., Stephenson, F.R., 1977a, Mon. Not. R. astr. Soc., 179, 87p-92p

Clark, D.H., Stephenson, F.R., 1977b, Historical Supernovae, Perqamon Press, Oxford

Clifton, T.R., Lyne, A.G., 1986, Nature, 320, 43-45

Danziqer, I.J., Goss, W.M., 1980, Mon. Not. R. astr. Soc., 190, 47p-49p

Duin, R.M., Strom, R.G., 1975, Astr. Astrophys., 39, 33-42

Gorenstein, P., Seward, F., Tucker, W., 1983, in IAU symp. 101: Supernova Remnants and Their X-ray Emission, ed. P. Gorenstein and I.J. Danziqer, D. Reidel, Dordrecht, p.1-15

Green, D.A., 1987, A Catalogue of Galactic Supernova Remnants, version IV.1, Mullard Radio Astronomy Observatory, Cambridge, U.K.

Groth, E.J., 1975, Astrophys. J. Suppl. Ser., 29, 453-465

Gull, S.F., 1975, Mon. Not. R. astr. Soc., 171, 237-242

Helfand, D.J., Becker, R.H., 1985, in: Crab Nebula and Related Supernova Remnants, ed. R.B.C. Henry and M.B.C. Kafatos, Cambridge, p.241-245

Helfand, D.J., Chance, D., Becker, R.H., White, R.L., 1984, Astr. J., 89,819-823

Higdon, J.C., Lingenfelter, R.E., 1980, Astrophys. J., 239, 867-872

Lamb, R.C., Markert, T.H., 1981, Astrophys. J., 244, 94-101

Lozinskaya, T.A., 1979, Sov. Astr., 23, 506-507

Lyne, A.G., Manchester, R.N., Taylor, J.H., 1985, Mon. Not. R. astr. Soc, 213, 613-639

Maceroni, C., Salvati, M., Pacini, F., 1974, Astrophys. Sp. Sci., 28, 205-212

Manchester, R.N., Durdin, J.M., Newton, L.M., 1985, Nature, 313, 274-376

Manchester, R.N., Taylor, J.H., 1977, Pulsars, Freeman, San Fransisco

Matsui, Y., Long, K.S., Dickel, J.R., Greisen, E.W., 1984, Astrophys. J., 287, 295-306

Miller, G.E., Scalo, J.M., 1979, Astrophys. J. Suppl. Ser., 41, 513-547

Milne, D.K., 1971, Aust. J. Phys., 24, 757-767

Narayan, R., 1987, Astrophys. J., 319, 162-179

Ostriker, J.P., Gunn, J.E., 1971, Astrophys. J., 164, L95-L104

Pacini, F., 1972, in: The Physics of Pulsars, Ed. A.M. Lenchek, Gordon and Breach, London, p.119-134

Pacini, F., Salvati, M., 1973, Astrophys. J., 186, 249-265

Radhakrishnan, V., 1982, Contemp. Phys., 23, 207-231

Radhakrishnan, V., Srinivasan, G., 1980 , J. Astrophys. Astr., 1, 25-32

Radhakrishnan, V., Srinivasan, G., 1982, Curr. Sci., 51, 1096-1099

Radhakrishnan, V., Srinivasan, G., 1984, in: Proceedings of the 2nd Asia-Pacific Regional Meeting in Astronomy (Bandung, 1981), ed. B. Hidayat and M.W. Feast, p.423-431

Reynolds, S.P., Chevalier, R.A., 1984, Astrophys. J., 278, 630-648

Srinivasan, G., Bhattacharya, D., Dwarakanath, K.S., 1984, J. Astrophys. Astr., 5, 403-423

Srinivasan, G., Dwarakanath, K.S., 1982, J. Astrophys. Astr., 3, 351-361

Stokes, G.H., Segelstein, D.J., Taylor, J.H., Dewey, R.J., 1986, Astrophys. J., 311, 694-700

Strom, R.G., Goss, W.M., Shaver, P.A., 1982, Mon. Not. R. astr. Soc., 200, 473-487

Tammann, G.A., 1982, in: Supernovae, a Survey of Current Research, ed. M.J. Rees and R.J. Stoneham, p.371-403

Trimble, V., 1983, Rev. Mod. Phys., 55, 511-563

van den Heuvel, E.P.J., 1984, J. Astrophys. Astr., 5, 209-233

Vivekanand, M., Narayan, R., 1981, J. Astrophys. Astr., 2, 315-337

Weiler, K.W., 1983, in IAU Symp. 101: Supernova Remnants and Their X-rav Emission, ed. P. Gorenstein and J. Danziger, D. Reidel, Dordrecht, p.299-320

Weiler, K.W., 1985 , in: Crab Nebula and Related Supernova Remnants, ed. R.B.C. Henry and M.B.C. Kafatos, Cambridge, p. 227-239